# OPTIMIZATION BASED CONTROL SYSTEMS TO IMPROVE PERFORMANCE OF EXOSKELETONS

SAI KIRAN GUNTI

Bachelor of Technology in Mechanical Engineering

Jawaharlal Nehru Technological University

May 2015

Submitted in partial fulfillment of requirements for the degree

MASTER OF SCIENCE IN MECHANICAL ENGINEERING

at the

CLEVELAND STATE UNIVERSITY

August 2021

We hereby approve this thesis for

SAI KIRAN GUNTI

Candidate for the Master of Science in Mechanical Engineering degree for the

Department of Mechanical Engineering

and the CLEVELAND STATE UNIVERSITY'S

College of Graduate Studies by

________________________________________

Dr. Antonie van den Bogert,
Thesis Chairperson
Department of Mechanical Engineering

________________________________________

Dr. Eric Schearer,
Thesis Committee Member
Department of Mechanical Engineering

________________________________________

Dr. Ryan Farris,
Thesis Committee Member
Department of Mechanical Engineering

Date of Defense: August 2, 2021

# ACKNOWLEDGMENTS

I would like to thank all my friends and family for their help and support in my completion of this thesis. First and foremost, many thanks to my advisor Dr. Ton van den Bogert for giving me an opportunity to research in this field. Thank you so much for your patience, guidance, and support. Your explanations and technical expertise are greatly appreciated. I have learned a lot under your guidance.

I would like to thank my committee members, Dr. Eric Schearer, Dr. Ryan Farris, and Professor Bogdan Kozul for participating on my committee and for offering their valuable time and feedback on my thesis defense and also inspiring me in many ways, directly and indirectly. Thanks to Dr. Schearer for teaching me the fundamentals of controls and showing me the path towards the advanced control systems. Thanks to Dr. Farris for his role in the research and development of the Indego exoskeleton that provided me with the foundation for my research. Thanks to Professor Kozul for endless motivation, support and guidance throughout my journey at CSU and for mentoring me in countless ways.

I also want to thank the Parker Hannifin Corporation for loaning us the Indego exoskeleton for this research. Dr. Ryan Farris and Dr. Skyler Dalley, thank you for all your support with the Indego.

Thank you to all my HMC lab mates for all the support and fun: Huawei, Hala, Nicole, Dana, Farbod, Jen, Chris, and Roemer. Also, thanks to all faculty and members of the CHMS for all the seminars that showed the latest research in the field and for making the lab environment fun and engaging, even throughout COVID times.

I would also like to thank the Motion Technology Center at Parker Hannifin for hiring me and developing my skills as a Controls Engineer.

Thanks to Bogdan, my brother Sri Charan and my friend A. D. for pushing me to take the thesis option in the master’s program, as it made me understand more about doing research and gain all this knowledge. Thank you so much to my mothers Kalyani and Yamuna. Thank you so much to my best friend, Anusree, for all the help and support during research, testing, and writing this thesis.

Special thanks to my soon-to-be wife, Hannah, who played an important role in my completing this degree and for bearing with me throughout this journey.

This thesis is in memory of my deceased father, Gunti Venkata Ramana.

OPTIMIZATION BASED CONTROL SYSTEMS TO IMPROVE

PERFORMANCE OF EXOSKELETONS

SAI KIRAN GUNTI

## ABSTRACT

Advancements in control systems and optimization can potentially be used to enhance the performance of exoskeletons and prostheses in various aspects, such as to improve balance control and gait adaptation. These are the two aims of this thesis.

Aim 1 is to improve the balance of an underactuated exoskeleton with full-state feedback. The exoskeleton was modeled as a three-link inverted pendulum with passive stiffness at the ankle and controlled actuations at its other two joints. Though the system has no controlled actuation at its pivot, the system could be stabilized at its equilibrium point by a linear quadratic regulator (LQR) at the other two actuated joints to maintain the upright position against small perturbations. The feedback control parameters were then optimized to further improve the stability of the system.

Aim 2 is to improve the gait adaptation in exoskeletal walking. A control strategy based on human-in-the-loop optimization is presented in this thesis. This controller allows the exoskeleton to adapt to the changes in gait pattern and walking speed by optimization of the cost function based on muscle activation and ground reaction force. Simulation and real-time test experimental results of this adaptive controller are shown in this thesis.

TABLE OF CONTENTS

LIST OF TABLES

LIST OF FIGURES

# CHAPTER I

# INTRODUCTION

## 1.1 Background

For over a century, technologists and scientists have actively sought the development of exoskeletons and orthoses designed to augment human strength and endurance. While there are still many challenges associated with exoskeletal and orthotic design, advances in the field have been truly impressive [1].

An exoskeleton can be described as a system consisting of an external skeleton with a mechanical structure, integrated with actuators, sensors, control elements, and sometimes elastic components that assist or augment the performance of the wearer. The origin of exoskeletons date back to 1890, where an exercising apparatus, as shown in Figure 1, was designed specifically to augment lower-limb mobility for conditioning the cardio-vascular system and for training agility, or for the coordination of movements involving exercising the arms by simultaneously exercising both arms and legs [2].

An exoskeleton works in parallel or sometimes in series with humans, assisting the performance of various tasks. Exoskeletons can be further classified into multiple categories based on design, purpose, and actuation, such as: series and parallel exoskeletons, upper limb and lower limb exoskeletons, passive and powered exoskeletons, rehabilitation and assistive exoskeletons, and power-assisting and power-augmented exoskeletons. Some of these classifications are detailed below.

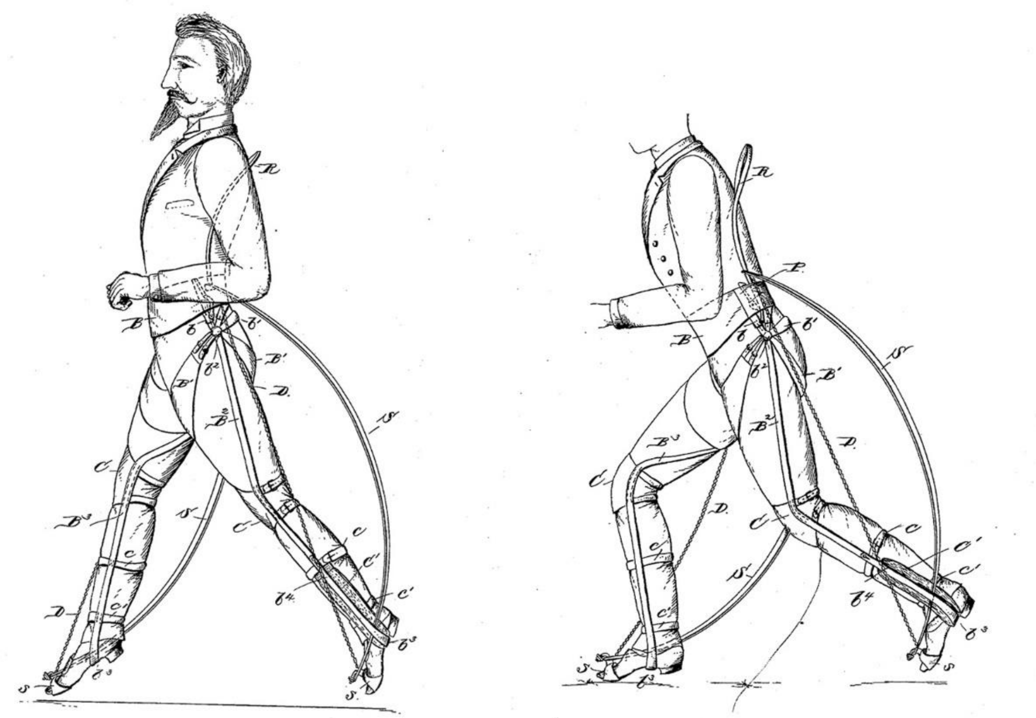

*Figure 1: Nicholas Yagn's apparatus for facilitating walking, running, and jumping [2].*

Series exoskeletons are mostly used to improve the performance of the wearer by increasing running speed or jump height. Also, studies have shown that these series exoskeletons can reduce the metabolic cost of running by lowering impact losses and providing energy return [1] [3]. Figure 2 shows some notable examples of series exoskeleton devices. In contrast, parallel exoskeletons act in parallel with humans for load transfer or assisting purposes. Examples of parallel exoskeletons are shown in Figure 3.

Passive exoskeletons do not use external power or actuation but use springs, dampers, or elastic materials that can store energy from human movements and release it when required [4]. These passive exoskeletons are mostly used for applications involvin

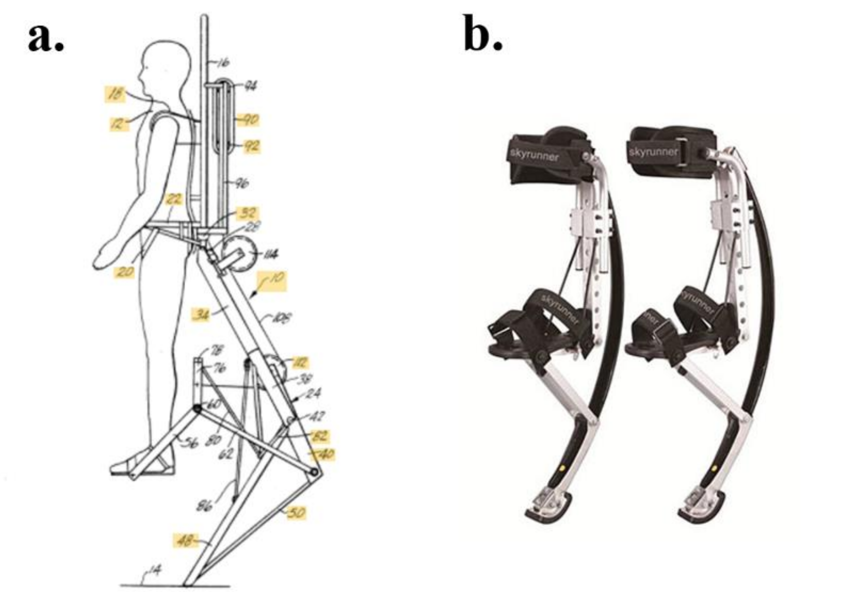


*Figure 2: Series exoskeleton examples. a. Human bipedal locomotion device [3]; and b. Skyrunner running and bouncing stilts [5].*

weight redistribution, energy capture, damping shocks or vibrations, and also in some locking mechanisms [6]. Active exoskeletons are powered by electromechanical, hydraulic, or pneumatic actuators based on applications. There was also research done on quasi-passive exoskeletons, where the stiffness of the passive exoskeleton can be varied based on requirement or performance [7].

In this thesis, we focused on lower-limb-powered prosthesis exoskeletons developed to assist individuals with loss of mobility from several causes, including spinal cord injuries, paraplegia, stroke, and similar conditions. There are about 296,000 people with spinal cord injury (SCI) in the United States alone as of 2021, and around 40% of these cases result in paraplegia [8]. Individuals with such disabilities in mobility face difficulty in moving and have a reduced quality of life. The average remaining years of life for persons with SCI have not improved since the 1980s and remain significantly below life expectancies of persons without SCI [8].

In recent years, many exoskeletons have been developed to assist individuals by improving their mobility and helping in rehabilitation. Various powered exoskeletons and orthoses for the lower limbs have been developed and were released into the market, such as the Indego exoskeleton by Parker Hannifin [9] and the ReWalk exoskeleton [10]. Also, other exoskeletons have been developed at universities, such as the portable exosuit developed at Harvard University [11] and the BLEEX developed at the University of California, Berkeley [12]. These exoskeletons usually help humans to perform a particular task. Some common tasks include rehabilitation training, where exoskeletons are used with individuals with neurological or orthopedic damage as assistive devices to help extend or improve their walking capabilities in day-to-day life, and as work support for healthy users in applications such as load carrying and military purposes.

Both exoskeletons and prosthetic devices have a mechanical structure integrated with actuators that can replace or assist the limb joints in performing a task, such as walking or rehabilitation based on a specific requirement. Electric motors are the most-used actuators, and in some cases, exoskeletons are powered by hydraulic systems [13]. Various exoskeletons and prosthetics are illustrated in Figure 3.

### 1.2 Motivation and Research Goals

Though many advanced control systems are in development to control actuators for various purposes, the existing exoskeletons still need further development for better control. Many exoskeletons have a jerky motion, and users still need crutches to balance

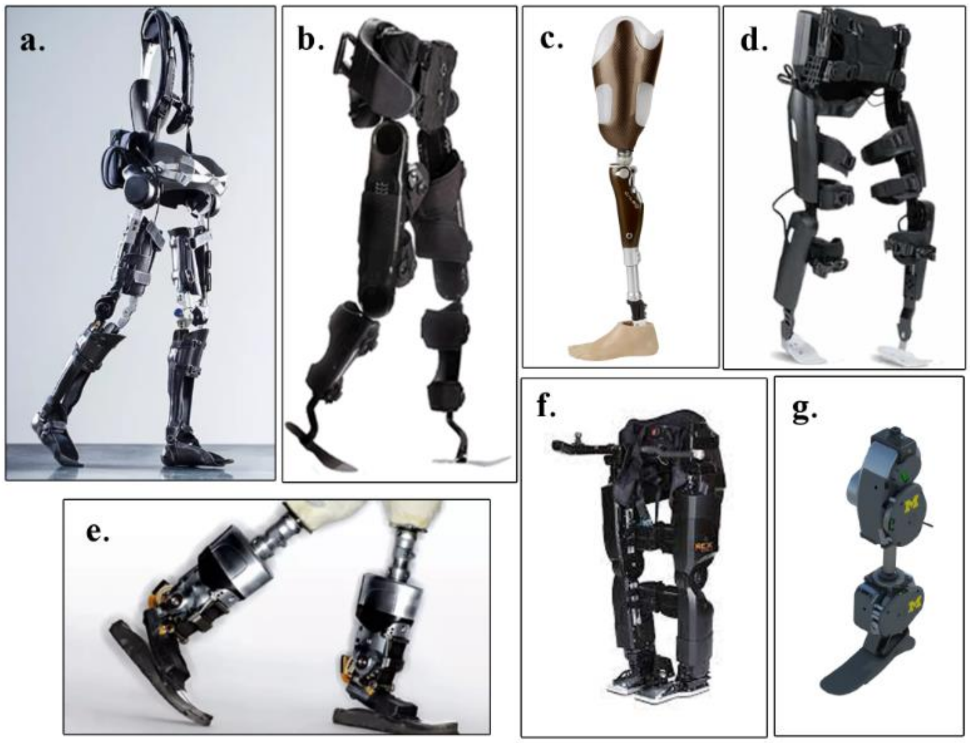


*Figure 3: Existing Powered Exoskeletons and Prosthetics. a. PHOENIX Medical Exoskeleton (SuitX); b. INDEGO (Parker Hannifin); c. C-Leg (Ottobock); d. Rewalk Personal 6.0 (ReWalk); e. Bionic Leg (MIT); f. REX (ReBionics); and g. Open-source Bionic Leg (UMich)*

themselves. Also, many of these exoskeletons use a fixed reference for the control system, which might not be suitable for all users.

Though researchers work to improve performance and control of exoskeletons and prosthetics and many research papers are published on developing control strategies for exoskeletons, there is still a need for further research to improve control for exoskeletons and prosthetics. One of the greatest challenges in exoskeleton control is related to the continuous motion profile adaptation of the exoskeleton. As many exoskeletons are given a fixed-reference trajectory [14] [15], these exoskeletons are unable to react to a change in walking pattern. Motion planning is one of the biggest challenges in exoskeleton controls.

Also, most of the current exoskeletons are designed and developed for people with paraplegia or other disabilities where the individual will rely entirely on the gait of the exoskeleton to achieve movement of the limbs. The control system is therefore not crucial in the performance of these types of exoskeletons, as it is usually a fixed-gait cycle, and the exoskeleton does not need to cooperate with human muscles. Limited research is available on powered exoskeletons working synchronously with able-bodied individuals, such as those with incomplete spinal cord injuries, stroke patients, and individuals with cerebral palsy, where better controls are needed for smooth cooperation between the user and the exoskeleton.

It is also known that exoskeletons do not have good balance support. It is left to the individuals to balance, and sometimes they must rely on crutches for that balance. Also, some exoskeletons do not have an actuator at the ankle, which makes the device easier to use but limits the controls to assist with the balance of the exoskeleton. Improving the balance of exoskeletons by using advanced control strategies is advantageous for a wide range of applications. The need for exoskeletons is not limited to individuals with disabilities, but may also help aging individuals decrease risk of falls.

Aging increases the risk of falls and is associated with injuries. Approximately one-third of community-dwelling older adults fall each year, and 11% of these falls result in serious injury [16]. Aging is also associated with decreased lower extremity strength.

This decline in strength could impair the ability to respond quickly and forcefully to prevent falling after a postural disturbance, leading directly to increased falling in older adults [17].

This research was conducted to explore control theory in improving the balance of the exoskeleton using control algorithms and to provide solutions to certain limitations of exoskeleton capabilities. Also, these limitations are particularly important when the exoskeletons are used by able-bodied individuals. This research also explored control algorithms to improve exoskeleton compatibility with able-bodied individuals to solve certain existing motion planning problems associated with walking.

### 1.3 The Indego Exoskeleton

The Indego exoskeleton [9] by Parker Hannifin (shown in Figure 3[b]) was used in this research to test designed control algorithms. Indego is a powered, lower-limb orthosis, and it is the lightest exoskeleton commercially available [18]. The Indego enables individuals with mobility impairments to stand and walk and is currently used by individuals with spinal cord injury levels T3-L5.

The Indego's design and controls were based on the research done by Farris et al. [15] [19] [20], which endeavored to provide gait assistance to individuals with spinal cord injuries. This exoskeleton has four electric motors that provide actuation at right and left hip and knee joints through speed reduction transmissions [19]. The control structure for this exoskeleton consists of variable-impedance controllers at joint level, supervised by an event-driven, finite state controller. This controller consists of variable gain proportional-derivative (PD) feedback controls at each actuated joint.

For personal or commercial use, the Indego exoskeleton is used with an iOS application. This application lets the user track progress and performance data [21]. For research purposes, the Indego can be operated and controlled using MATLAB/Simulink in real time. CAN serves to establish communication between the Simulink Desktop Real-Time and the Indego exoskeleton, where packets of data can be exchanged between them. This technology enables researchers to develop and test new and advanced control strategies and algorithms to further the development of controls for the Indego.

The MATLAB/Simulink model provided by Parker Hannifin to operate and control the Indego for research is shown in Figure 4. This model inputs various statistics and feedback data such as position, velocity, current, and temperature data from encoders and embedded probes and sends joint reference trajectories, values for feedback control gains, and current control parameters to the Indego exoskeleton CAN messages in the communication channel. Figure 5 shows the model inside the Position Control Parameters subsystem block from Figure 4, where the reference and control parameters are sent through CAN communication.

### 1.4 Thesis Organization

The main goals of this thesis were to develop control algorithms that improve the motion planning of the exoskeleton for gait assistance and improve the balance of the exoskeleton. The remainder of this thesis consists of three chapters.

Chapter 2 addresses solutions that improve balance in exoskeletons. Aim 1 focuses on balance controls in the exoskeletons. The emphasis of this chapter is simulation-based design of a control system to improve the balance of an exoskeleton. As discussed, exoskeletons are limited by controls to help improve balance. In this thesis, the exoskeleton is considered as a three-link, inverted pendulum model with passive

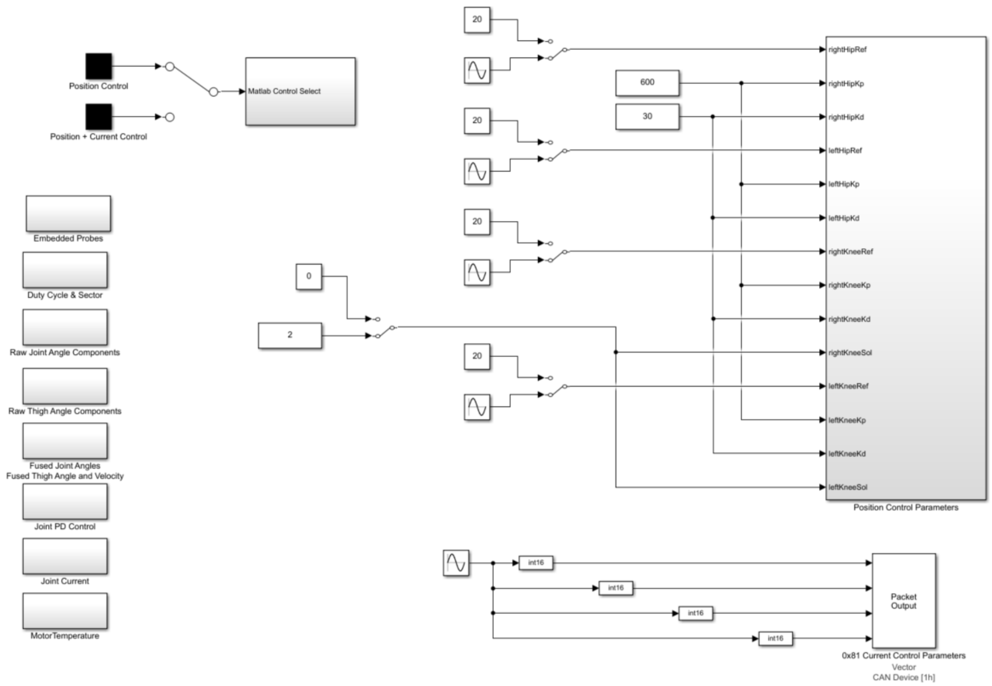


*Figure 4: Simulink model provided by Parker Hannifin for research in controls.*

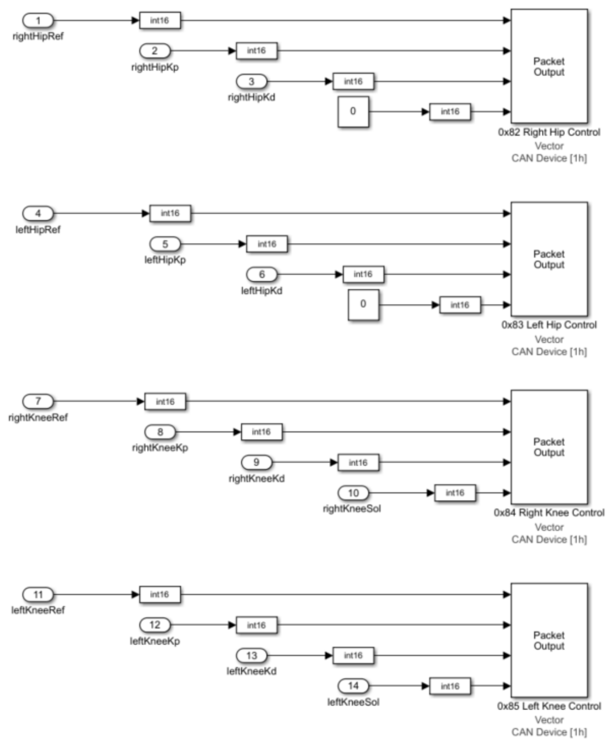


*Figure 5: Packet Output blocks sending data to Indego exoskeleton through CAN communication.*

stiffness at the ankle and equations of motion are derived from this model. The control system is developed to balance the exoskeleton. The control parameters are optimized to improve controller performance.

Chapter 3 addresses solutions to the adaptation of the gait cycle. This chapter aims to design, simulate, and test a controls strategy that will improve the motion planning of the exoskeleton by adapting to changes in the gait cycle. This motion planning was performed by adapting the gait cycle command signal given to the exoskeleton based on the parameters of the optimizer. The optimizer minimizes the cost function based on muscle activation and makes adjustments to the gait cycle.

Chapter 4 discusses the outcomes of this thesis and possible avenues for future research.

# CHAPTER II

# BALANCE CONTROL IN THE UNDERACTUATED INDEGO EXOSKELETON

## 2.1 Introduction

Posture control in the human body uses a complex feedback control strategy governed by its central nervous system (CNS). The CNS has complex patterns of muscle activation to balance the human body and reduce the risk of falling. Every year, thousands of people are hospitalized as a result of injuries from falls, and about 30% of injured people are re-hospitalized one or more times during any given year following the injury [8]. This demonstrates the need for research in controls to improve balance in exoskeletons, which has the potential to help people not only by assisting them in walking, but also by improving their balance and stability.

As most exoskeletons still lack balance, users require crutches to balance themselves. However, recent advancements have provided an intuitive understanding of the modeling and controls of dynamic systems, which can be used to design a controls strategy that helps solve balance problems.

With underactuated systems, it is especially challenging to design controls that improve balance. The Indego exoskeleton has actuators at its hip and knee joints, but it does not have an actuator at its ankle joint [9]. This limits its balance capabilities. Apart from the Indego, other systems in industrial, medical, and space environments may have fewer actuators than their degree of freedom. There are many low-ordered, laboratory underactuated systems, such as the Pendubot, the Acrobot, the Furuta pendulum, the Kapitza pendulum, and the pendulum on a cart for which controllers are developed [22]. The concept of controlling the balance of the exoskeleton using its dynamics is similar to the technique used in acrobatics, where performers use the swing-up moment to perform a flip on a high bar, but not the torque at the pivot. Also, a person walking on stilts can balance in an upright position through movement in the knees, though there is no actuation at the foot of the stilt.

To improve balance in exoskeletons and humanoid robots, linear inverted pendulum models and control schemes have been used [23]. In recent studies, humanoid robot balance was improved by using a spherical inverted pendulum model for standing balance control in a biped [24]. Also, a balance control method for position control-based robots was proposed by describing the dynamic characters of the robot using a linear inverted pendulum plus flywheel model [25]. In this thesis, a model-based controller was developed for balancing the Indego exoskeleton based on the dynamics of a three-link inverted pendulum.

### 2.2 Dynamic Modeling of a Three-Link Inverted Pendulum

The exoskeleton was modeled as a three-link inverted pendulum. The three links represent the shank, thigh, and hip sections of the exoskeleton. As shown in the linkage diagram in Figure 4, $\theta_a$, $\theta_k$, and $\theta_h$ are the angles at the ankle joint, knee joint, and the hip joint, respectively. Variables $m_s$, $m_{th}$, and $m_h$ are the masses of shank, thigh, and trunk links, respectively. $I_s$, $I_{th}$, and $I_{tr}$ are the moments of inertia of the shank, thigh, and trunk links, respectively. The exoskeleton was considered here as a system with uniform straight links with lengths of shank, thigh, and hip as $l_s$, $l_{th}$ and $l_{tr}$, where hip and knee joints are actuated by torque motors, with no actuation at the ankle joint. A passive stiffness was considered at the ankle joint to model the connection between shank and foot plate in the Indego exoskeleton. The schematic representation of the underactuated exoskeleton considered as the three-link inverted pendulum is shown in Figure 6, and the model properties are listed in Table 1.

| | Length | mass | Moment of inertia | Location of center of mass |
|---|---|---|---|---|
| Shank | 0.45 m | 4.53 kg | 0.13 kg.m$^2$ | 0.25 m |
| Thigh | 0.45 m | 8.16 | 0.32 kg.m$^2$ | 0.35 m |
| Trunk | | 20.41 | 3.83 kg.m$^2$ | 0.35 m |

*Table 1. Model properties for the three-link inverted pendulum*

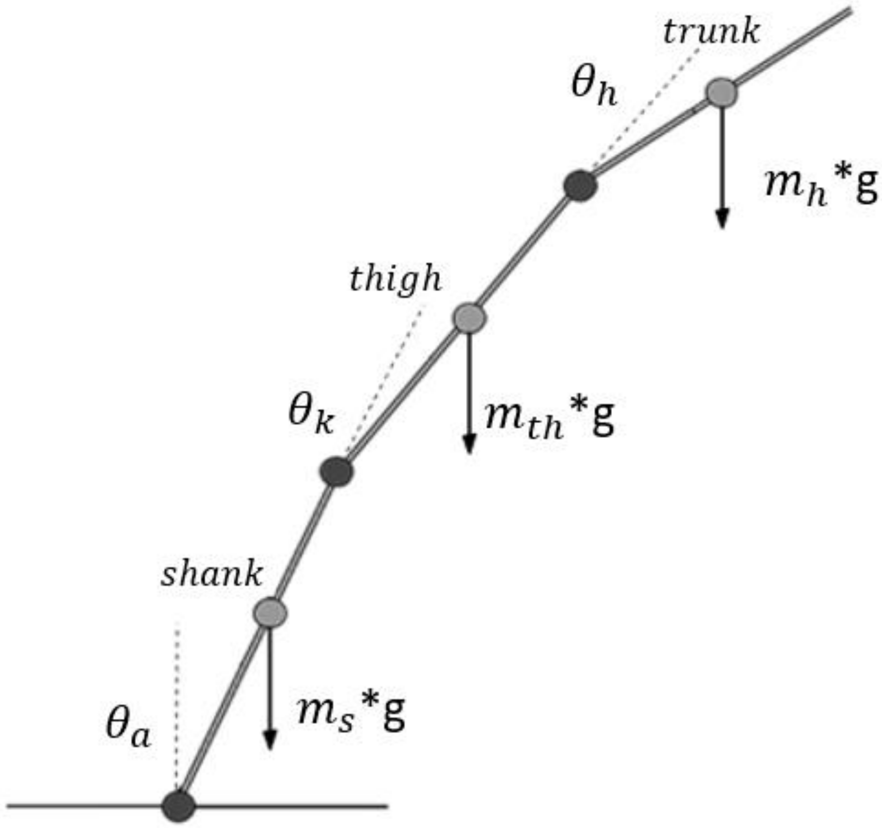


*Figure 6: Linkage diagram of the three-link inverted pendulum model.*

The equations of motion can be generated in multiple ways that give the same results [26]. In this thesis, the equations were derived with the Lagrange approach. In Lagrangian mechanics, the trajectory of a system of particles is derived by solving the equations of motion, which are the Lagrange equations in two forms. Lagrange equations of the first kind treat constraints explicitly as extra equations, often using Lagrange multipliers. The Lagrange equations of the second kind incorporate the constraints directly using the judicious choice of independent generalized coordinates [27]. The Lagrangian function ($L$) is defined as $L = T - V$, which summarizes the dynamics of the entire system, where *V* is the total potential energy of the system, and *T* is the total kinetic energy of the system [28]. The Lagrange equations of the second kind are derived as follows:

$$\frac{d}{dt}\left(\frac{\partial L}{\partial \dot{q}_j}\right) - \frac{\partial L}{\partial q_j} = \tau_j \qquad (2.1)$$

where $\tau$ is the joint torques, $j = 1, 2, \ldots$ represents the j[th] degree of freedom, $q_j$ is the generalized coordinates, and $\dot{q}_j$ is the generalized velocities [29]. The Lagrangian equations for the underactuated exoskeleton Indego, which was modeled as a three-link inverted pendulum, were defined in MATLAB using the symbolic toolbox to calculate the symbolic expressions for the equations of motion. Appendix shows the MATLAB code used to generate the equations of motion. The resulting equations of motion can be written as follows:

$$M(q)\ddot{q} + G(q,\dot{q}) = \tau \qquad (2.2)$$

where *M* is the mass matrix, and *G* represents gravity, centrifugal, and Coriolis effects.

**2.3 Designing Controls for the Underactuated Exoskeleton System**

Controlling the underactuated system is a challenging task, as it possesses nonlinear terms. To solve these nonlinear terms, we linearize the system at a fixed point or equilibrium point, and then design the controller for that linear system. To further solve for the multibody dynamic equations of the underactuated exoskeleton, the three-link inverted pendulum was modeled using state space equations. Let *X* be the vector of state variables for this system, which is defined as follows:

$$X = (q, \dot{q})^T \quad (2.3)$$

The state space equations of this nonlinear system using the above-defined state variables are given as follows:

$$\dot{X} = f(X, U)$$

where $f = \begin{bmatrix} \dot{q} \\ M(q)^{-1}\big(\tau - G(q, \dot{q})\big) \end{bmatrix}$ which is a 6 x 1 matrix *(2.4)*

$$\tau = \begin{bmatrix} -S\theta_a \\ u_k \\ u_h \end{bmatrix}$$

As this is an underactuated system and there is no actuator at the ankle joint, a passive ankle torque with stiffness *S = 200 Nm/rad* was added instead. Since this under-actuated system requires a full state feedback, it is not possible to stabilize the system using a traditional PD controller. A controller $U = \begin{bmatrix} u_k \\ u_h \end{bmatrix}$ is designed using linear quadratic regulator (LQR) theory.

The nonlinear equation 2.4 was linearized at its equilibrium point $x_o = (0,0,0,0,0,0)^T$ using a first-degree approximation of the Taylor series:

$$f(X, U) \approx AX + BU \quad (2.5)$$

where *A* and *B* are the Jacobian matrices $A = \frac{\partial f}{\partial X}$ , $B = \frac{\partial f}{\partial U}$ evaluated at the point $x_o$.

The calculated values are:

$$A = \begin{bmatrix} 0 & 0 & 0 & 1 & 0 & 0 \\ 0 & 0 & 0 & 0 & 1 & 0 \\ 0 & 0 & 0 & 0 & 0 & 1 \\ -168.3352 & -273.1057 & 5.9244 & 0 & 0 & 0 \\ 367.8850 & 582.6138 & -30.8644 & 0 & 0 & 0 \\ -206.6919 & -320.5858 & 55.9038 & 0 & 0 & 0 \end{bmatrix} \text{ and}$$

$$B = \begin{bmatrix} 0 & 0 \\ 0 & 0 \\ 0 & 0 \\ -2.0921 & 1.1097 \\ 4.4475 & -2.5552 \\ -2.5552 & 1.8073 \end{bmatrix}$$

It was assumed that the states and controls for this system were not bounded. Analyzing the above linearized system for its controllability showed that the linearized dynamics of the system related to the equilibrium position was controllable, and the system can be returned to its zero state in finite time if started away. An optimal feedback controller was designed for this linearized time invariant system's state space equation given in Equation 2.6 with a control law:

$$U = -K * X \tag{2.6}$$

where K is a 2 x 6 gain matrix of the designed optimal feedback controller with control gains in it. This gain matrix was used to control the two actuated joints to make the whole system stable at its equilibrium position with small perturbations.

This controller was initially designed by using the linear quadratic regulator (LQR) method. The LQR is a method used to optimally control a linear dynamic system at a minimum cost. The cost of the system is defined by a quadratic function [30]. This controller is often used for stabilizing inverted pendulum systems [31]. LQR is used to calculate the optimal gain matrix for continuous time systems around the operating point by minimizing the quadratic cost function, as in Equation 2.7, which is based on the system's state and control trajectories *X(t)* and *U(t)*:

$$J(K) = \int_0^{\infty} (X(t)^T Q X(t) + U(t)^T R U(t)) dt \tag{2.7}$$

where the error weighting matrix *Q* is a real, symmetric-positive, semi-definite matrix, and the control weighted matrix *R* is a real, symmetric-positive, definite matrix. The values used for Q and R are, Q = diag ([10 10 10 10 10 10]) and R = diag ([0.001 0.001]). These gains can be found in MATLAB using the inbuilt command shown in Equation 2.8, which gives us the gain matrix K solution for the Riccati equation S and the closed-loop eigenvalues e.

```
[K,S,e] = lqr(A,B,Q,R)
```
(2.8)

### 2.4 Simulation Results of the Underactuated Exoskeleton System

Based on the derived equations of motion, the dynamic modeling of the system was done in MATLAB for the underactuated exoskeleton modeled as a three-link inverted pendulum with passive stiffness at the ankle joint and actuators at the knee and hip joints. The response of the system without any controller starting at a zero position is shown in Figure 7, where it is clearly evident that the system is freely falling in response to gravity.

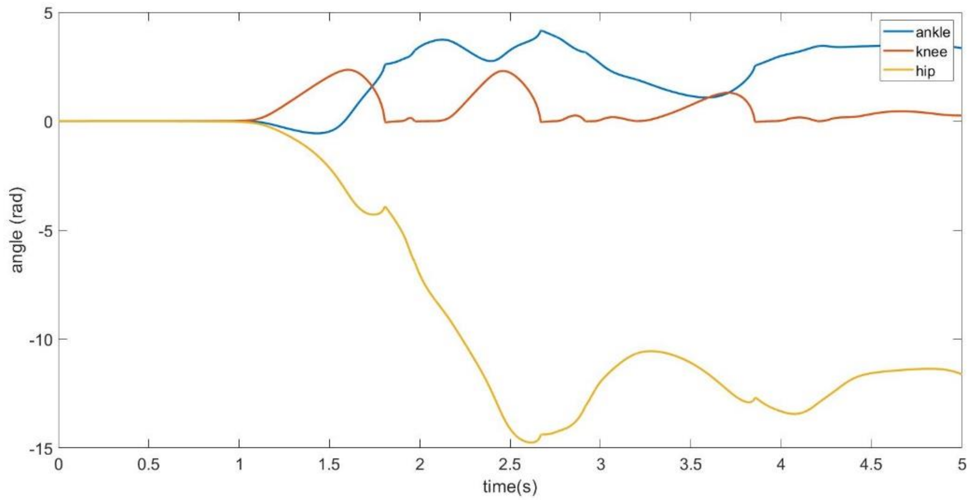


*Figure 7: Joint angle trajectory of the system without controller.*

After an optimal controller was designed using the LQR, the underactuated exoskeleton was simulated at various test cases to check the controllability range of the initial positions where the system was stable. The control gain matrix *K* obtained from the LQR command in MATLAB for the dynamic system is as follows:

$$K_{LQR} = \begin{bmatrix} 1590.64 & 1301.96 & 537.5 & 611.46 & 413.52 & 186.91 \\ -463.6 & -270.68 & 78.96 & -199.16 & -112.093 & -17.23 \end{bmatrix}.$$

For this given control gain matrix, the closed loop eigenvalues were obtained as follows:

$$e = [-78.025;\ -8.008;\ -2.023;\ -2.325;\ -4.886; -4.127]$$

This proves that the designed controller was stable, as all eigenvalues were negative. As the system was linearized at the equilibrium point, it is stable at $X = X_0$. When $X \neq X_0$, there is no proof to show the stability of the system, and hence simulation is needed to identify the range of stable points.

### *2.4.1 LQR Controller Test Case 1*

To test the performance of the designed controller, an arbitrary, nonzero initial condition $X(0)$ = [-0.1 rad;0;0;0;0;0] was given to check the response of the system. The joint angle trajectories for Test Case 1 of the simulations for this underactuated exoskeleton with closed loop response, using the LQR, is shown in Figure 8.

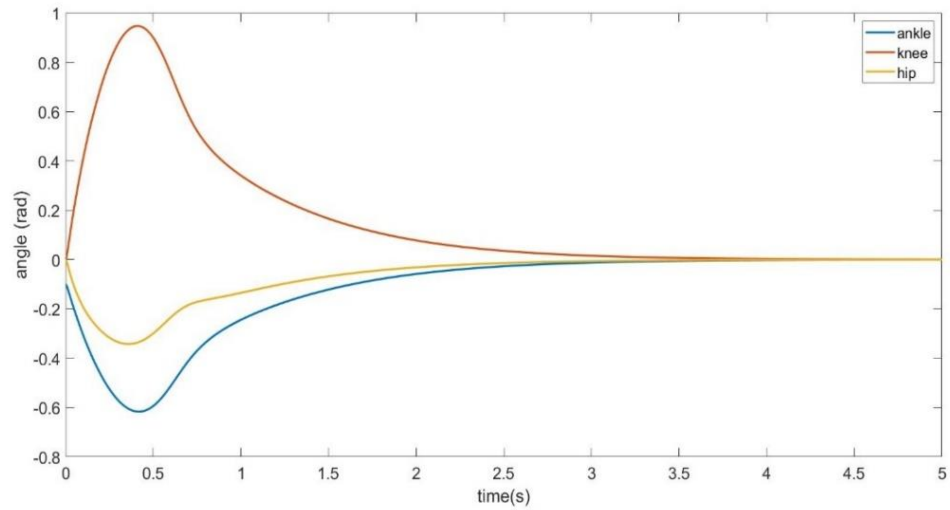


*Figure 8: Joint angle trajectories with non-zero initial position.*

The figure clearly shows that the system can be stabilized at the equilibrium position, even with a non-zero initial position. In order to stabilize, the knee joint has to move far from the origin to balance the three-link inverted pendulum, as it is underactuated. The torques at the hip and knee joints, as generated by the controller to stabilize the system, are shown in Figure 9.

### *2.4.2 LQR Controller Test Case 2*

To test the limits of the initial position where this controller can stabilize the system, multiple simulations were done. A peak point that this controller can stabilize

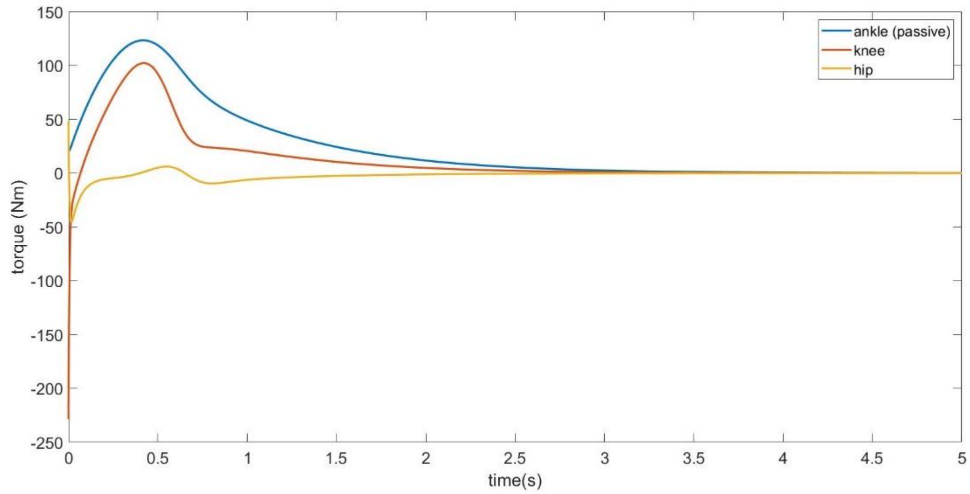


*Figure 9: Joint torques by controller in response to non-zero initial condition.*

was found at $X(0) = [-0.15; 0.23; -0.23; 0; 0; 0]$ radians, which is around 8-13 degrees of deflection from the equilibrium position. The joint angle trajectories for Test Case 2 are shown in Figure 10, and the torques generated by the actuators at knee and hip joints and passive stiffness at the ankle joint are shown in Figure 11.

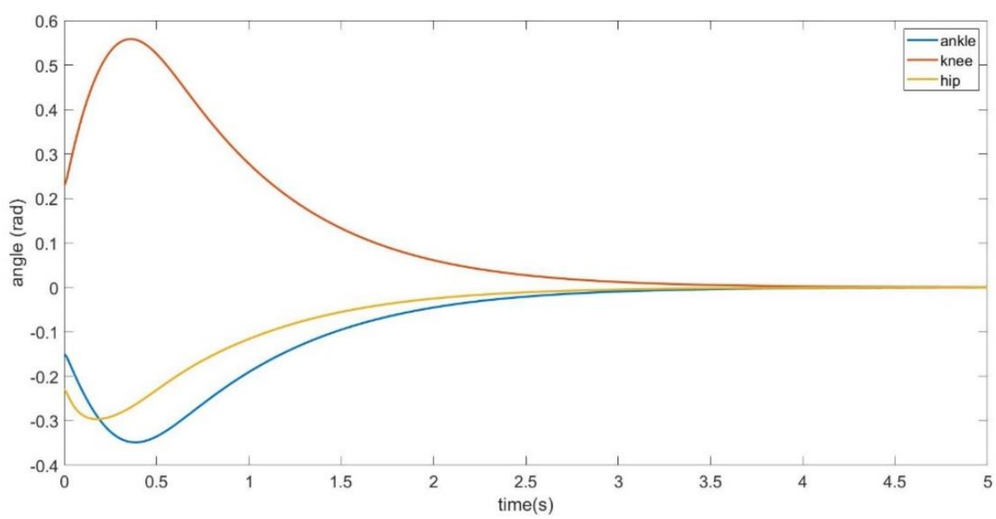


*Figure 10: Joint angle trajectories for LQR Test Case 2.*

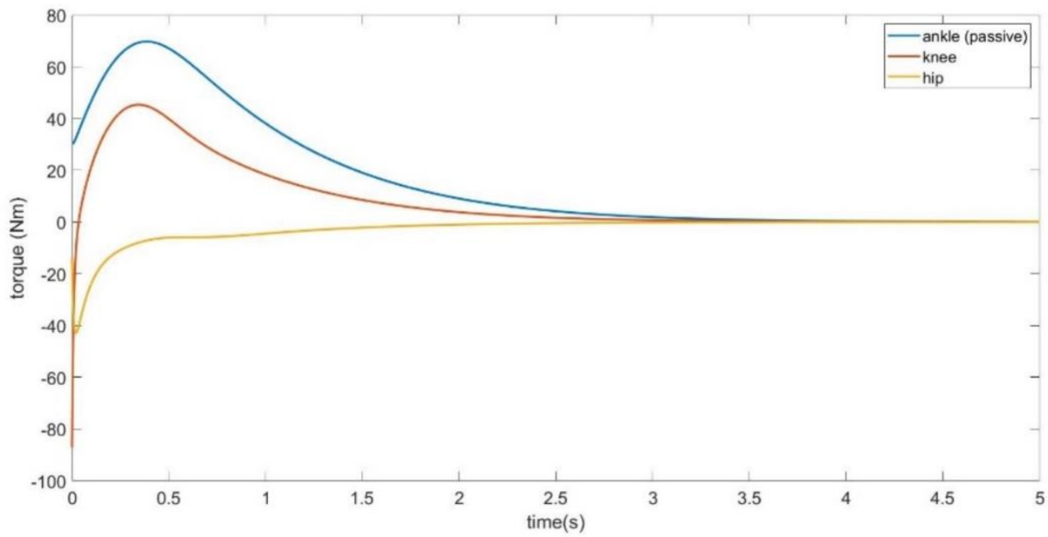


*Figure 11: Joint torques generated at the joints to stabilize the system.*

### 2.5 Optimization of Control Parameters

Though it is evident from the results shown above that the controller is stabilizing the system, it is possible to further improve the performance of the controller in such a way as to reduce overshoot and actuation torque at the joints. To improve the performance of the controller in the controllable range of initial positions, a grid of initial positions, a 10 x 10 x 10 grid with a range of initial positions from 0.2 to -0.2 radians, was made to simulate the system 1,000 times. Multiple iterations of these 1,000 simulations were done by an optimizer to find the controller gains *K* that minimize the LQR cost function.

$$J(K) = \sum_{grid\ points} \int_0^T X(t)^T Q X(t) + U(t)^T R U(t)\, dt \tag{2.9}$$

The optimization of the cost function was performed by using the Nelder-Mead simplex method, which is one of the most widely used methods for nonlinear, unconstrained optimization. The Nelder-Mead method attempts to minimize a scalar-valued nonlinear function of *n* real variables using only function values without any derivative information [32]. With the Nelder-Mead optimization method, a simplex is arranged by $n$ +1 test point sets for $n$ variables. Here, $n$ = 12 because $K$ is a 2 x 6 matrix. This simplex extrapolates the measured objective function at the test points to find and replace it with a new test point. This progression is performed by replacing the simplex with the worst point with a new simplex to see if it is better than the current point, and if it is better, stretching it in that direction. Otherwise, the previous simplex is shrunk towards the better point [33]. To effectively optimize this method, it is important to carefully choose the initial simplex.

We obtained 12 variables in the control gain matrix, as generated by the LQR, to stabilize the underactuated three-link inverted pendulum system as the initial simplex and the Q and R are the diagonal matrices where Q = diag ([10 10 10 10 10 10]) and R = diag ([0.001 0.001]). The response of the system with the designed controller is shown in Figures 10 and 11. Figure 12 shows the value of the cost function decreasing as the iterations progress to optimize the control variables for our system. The optimization was done for only 31 iterations, when the cost function reaches a user defined tolerance on the function value, in this case a positive scalar number 0.001, where the cost function was considerably reduced and the gain matrix still worked to stabilize the system.

Based on the optimized control parameters $K_{opt}$ from the Nelder-Mead simplex direct search, the system response was simulated from Test Case 2 to observe improvements. The joint angle trajectories and torques generated for the underactuated three-link inverted pendulum system are shown in Figures 13 and 14. The optimized control parameters $K_{opt}$ are given below:

$$K_{opt} = \begin{bmatrix} 1650.57 & 1357.48 & 536.76 & 615.84 & 428.42 & 187.98 \\ -497.95 & -197.23 & 76.44 & -220.51 & -112.59 & -17.53 \end{bmatrix}$$

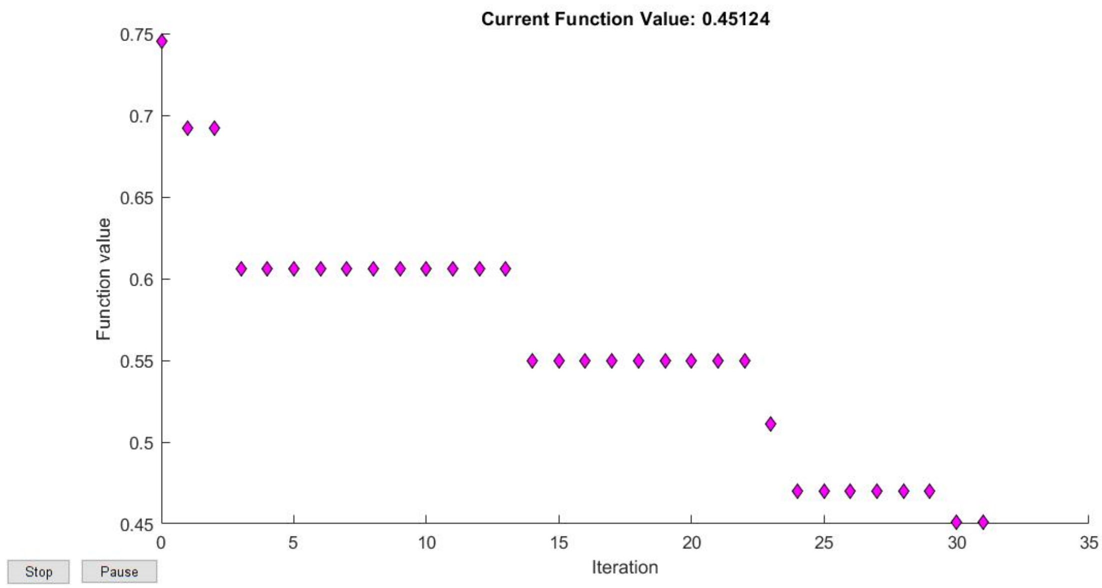


*Figure 12: Cost function decreasing during optimization.*

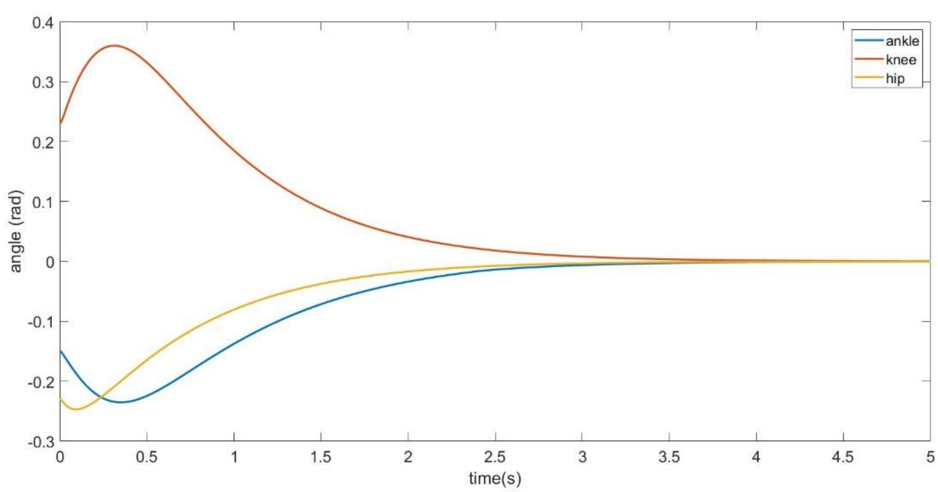


*Figure 13. Joint angle trajectories with the controller after optimization.*

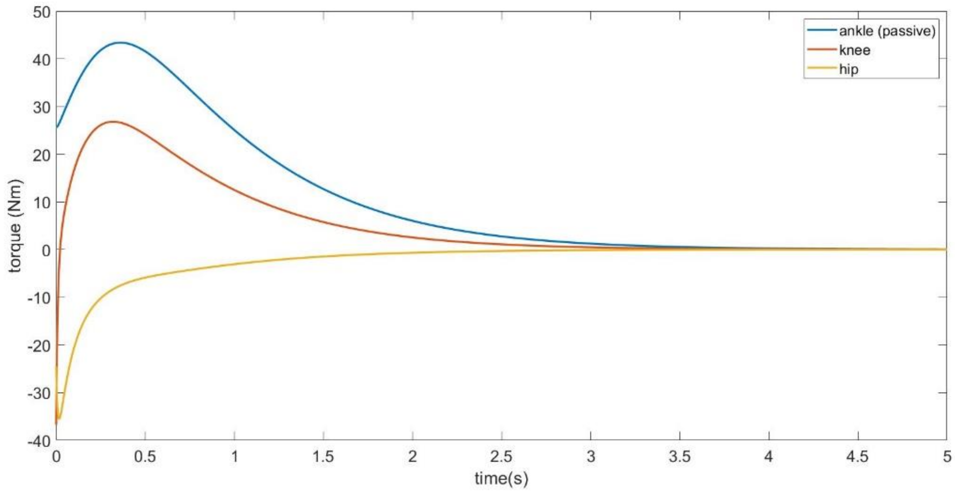


*Figure 14. Joint torques after optimization.*

Comparing Figure 13 with Figure 10, and Figure 14 with Figure 11, it is evident that after optimization of the control parameters, the performance of this dynamic system has improved considerably. The overshoot and the peak torque have been reduced considerably, which reduces the load on the motor to stabilize.

When the optimization was ran further till the default tolerance of 0.0001 is reached with default stopping criteria, the cost function is further decreased and the gain matrix still worked to stabilize the system but the movement had oscillations. The plot showing the decrease in cost function is shown in Figure15. The fully optimized control parameters $K_{fopt}$ are given below:

$$K_{fopt} = \begin{bmatrix} 1729.27 & 1380.23 & 515.59 & 634.42 & 406.83 & 187.63 \\ -535.54 & -193.81 & 73.94 & -201.81 & -108.81 & -17.74 \end{bmatrix}$$

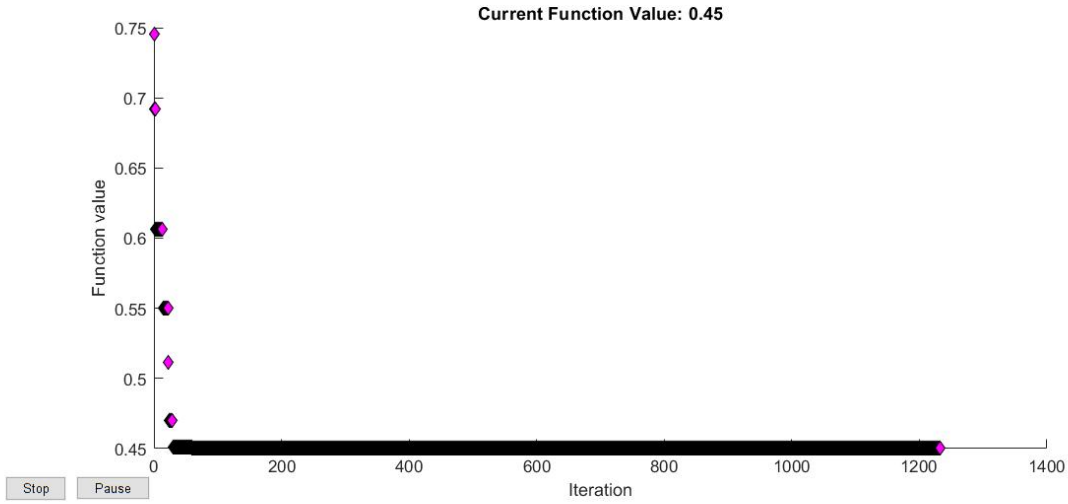


*Figure 15: Cost function decreasing while Optimization with default tolerances*

Based on the optimized control parameters $K_{fopt}$ from the Nelder-Mead simplex direct search with default tolerances, the system response was simulated from Test Case 2 to observe change in performance of the system. The joint angle trajectories and torques generated for the underactuated three-link inverted pendulum system are shown in Figures 16 and 17.

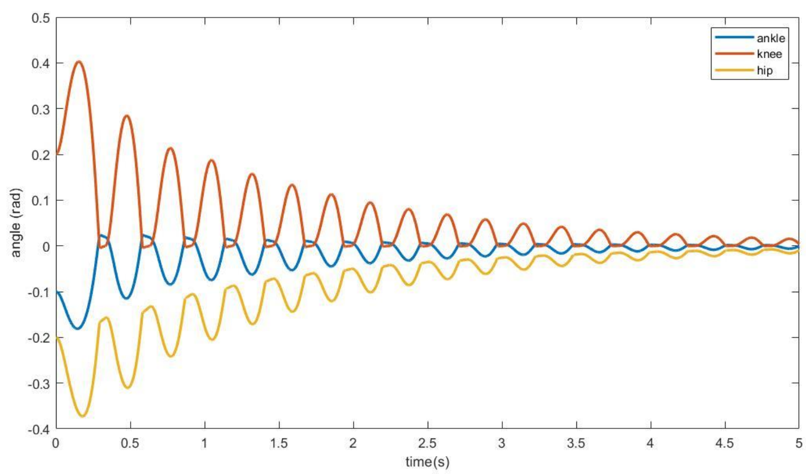


*Figure 16: Joint angle trajectories with the controller after optimization with default tolerances*

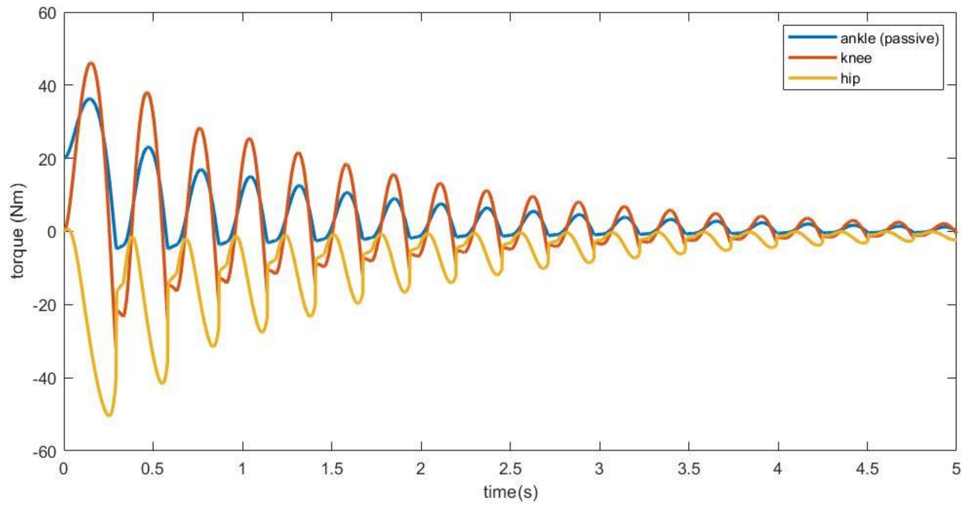


*Figure 17: Joint torques with the controller after optimization with default tolerances*

**2.6 Discussion**

In this chapter, a control algorithm was implemented to improve the balance of the underactuated Indego exoskeleton modeled as a three-link inverted pendulum using the Lagrange approach. As the Indego is an underactuated exoskeleton, a passive torque was added at the ankle, and the actuators at knee and hip were given torques by the controller to stabilize the system. The controller was designed using the LQR method to get the control gain matrix $K$ from Equation 2.6, as shown in Section 2.4. The simulation results using the $K$ gain matrix prove that the system can be stabilized at the equilibrium position with a non-zero initial position.

The $K$ gain matrix obtained from Equation 2.6 was further optimized using the Nelder-Mead simplex method to derive the new, optimized $K$ gain matrix, $K_{opt}$, shown in Section 2.5. The simulation results of the three-link inverted pendulum using this $K_{opt}$ shows a 25-30% decrease in the overshoot of the joint angles and around 25% less torque at the actuators to stabilize the system. Though the values of control gain matrices $K$ and

$K_{opt}$ are different, the difference is small and there is a large improvement in the system's performance. This indicates that it is a sensitive system, and the performance of the system can be influenced largely by changes in modeling and control parameters, and these can be studied further.

While the optimization method had better performance than the LQR method, it also had some limitations.  When the optimization was continued, oscillatory behavior was seen. This could possibly be avoided by increasing the weighting of the velocity terms in the cost function, by increasing the elements 5, 6, and 7 on the diagonal of the Q matrix.

The performance of the system also depends on the passive stiffness added at the ankle. Though the performance improves with the increase in stiffness, it might not work in reality, as an individual might fall if the center of pressures related to the ankle shifts beyond physical limits.

# CHAPTER III

# ADAPTIVE CONTROL FOR WALKING WITH THE INDEGO EXOSKELETON

## 3.1 Introduction and the Need for Adaptation

With the development of the latest technologies, exoskeletons are now widely used to support humans in many applications, such as rehabilitation, assistance, and augmentation. Most exoskeletons have a control system where fixed-joint angle trajectories are given as reference trajectories that they follow without adaptation [10] [14] [15]. This type of controls is suitable for applications where the exoskeleton is used to assist individuals with loss of mobility. In able-bodied individuals with partial or no loss of mobility, the gait pattern for each individual is different; and a standard gait reference trajectory as input to the exoskeleton might not be suitable for assistance.

In human walking, the coordination between joints is a dynamic and complex process controlled by the central nervous system (CNS). For able-bodied individuals walking with exoskeletons, the joint coordination is altered and controlled by two different controllers to perform the motion: the human CNS and the controller of the exoskeleton [34]. To perform normal walking with an exoskeleton, good coordination between these two controllers is required at the point where the controllers co-adapt to an equilibrium state. Without coordination between the human and the exoskeleton, the effectivity and efficiency of the exoskeleton's performance will not be maximal, making it harder for the user to walk.

Similar issues have been reported in powered prostheses. A recent study showed that there is a need to improve how powered prostheses are controlled and also how users are trained [35]. When the human tries to walk with a different gait pattern than the exoskeleton or prosthesis reference, there may also be an increase in muscle activation as the user and the robotic device "fight" each other.

In recent studies a power assist method was developed using an EMG-based feedback controller, where a phase sequence control method was implemented to maintain an assist ratio which is formulated based on the measured myoelectric signals. In this method by maintaining the assist ratio, the assistive power generated by the exoskeleton is controlled by adjusting assistive torques [36]. Also, in a different study, an approach for the cooperative controls of a hybrid system of a powered lower limb exoskeleton and functional electrical simulations (FES) is presented. The control structure consists of two control loops: a motor control loop and a muscle control loop, to minimize the motor torque contribution [37].

In this thesis, a new control algorithm with human-in-the-loop optimization was developed so the exoskeleton can adapt to different walking patterns that effectively reduce muscle effort.

### 3.2 Human-in-the-Loop Optimization for Gait Adaptation in the Indego

To automate the gait cycle adaptation while walking with the Indego exoskeleton, a model-based control algorithm using human-in-the-loop optimization was developed. This proposed algorithm can improve the user's walking experience by improving human and exoskeleton coordination. Previous research has shown that the human can be included in the optimization process where optimization methods were developed for identifying the torque patterns in real time, which can reduce the metabolic energy consumption by around 25% [38].

The inspiration of this type of optimization-based control comes from the techniques that humans use as they naturally optimize joint coordination patterns to perform various locomotory tasks, such as walking and running [39]. A recent study on optimizing both design and controls in lower limb prostheses showed that if the muscle crossing of the ankle is replaced with ideal motor torques that have identical kinematics, the human metabolic cost could be reduced by 41% [40]. There are several optimization algorithms that have demonstrated optimization of a single-gait parameter using gradient descent techniques. A qualitative comparison of these methods reveals the limitations due to noise and poor scaling; as in some methods, the steady-state cost mapping takes about an hour of walking and dynamic adaptation is not allowed [41]. A computer-based optimization of gait patterns that identifies energetically optimal cases working well in simulations of a simple biped model indicates that unusual gaits consume more energy and are tiring [42].

Though it is challenging to close the loop on human performance, a cost function, which quantifies the muscle activation effort or cost while the user walks with the exoskeleton, was derived based on muscle activations measured by electromyography (EMG) sensors over an *n* number of gait cycles. The muscle activation during walking was measured from the rectus femoris as it acts as a hip flexor, and its activity significantly changes with changes in speed [43]. When coordination between the exoskeleton and the user is low, the user will tend to work hard to walk, which increases muscle activations and hence the cost function also. When the user and the exoskeleton find equilibrium and work synchronously, muscle activation is reduced, and coordination is formed between the exoskeleton and the user.

This cost function can be optimized over a specified number of gait cycles in real time while the user walks with the exoskeleton. The controller based on this optimization will generate control parameters that will optimize the gait reference trajectory to the exoskeleton. These optimizer-generated parameters can allow a wide range of possible gait patterns to minimize the cost function. With a continuous optimization of these parameters, a best-possible gait pattern is approximated that lowers the cost function and shows the fewest muscle activations, and an equilibrium between the exoskeleton and the user is achieved. The block diagram for the human-in-the-loop gait adaptation algorithm is shown in Figure 18.

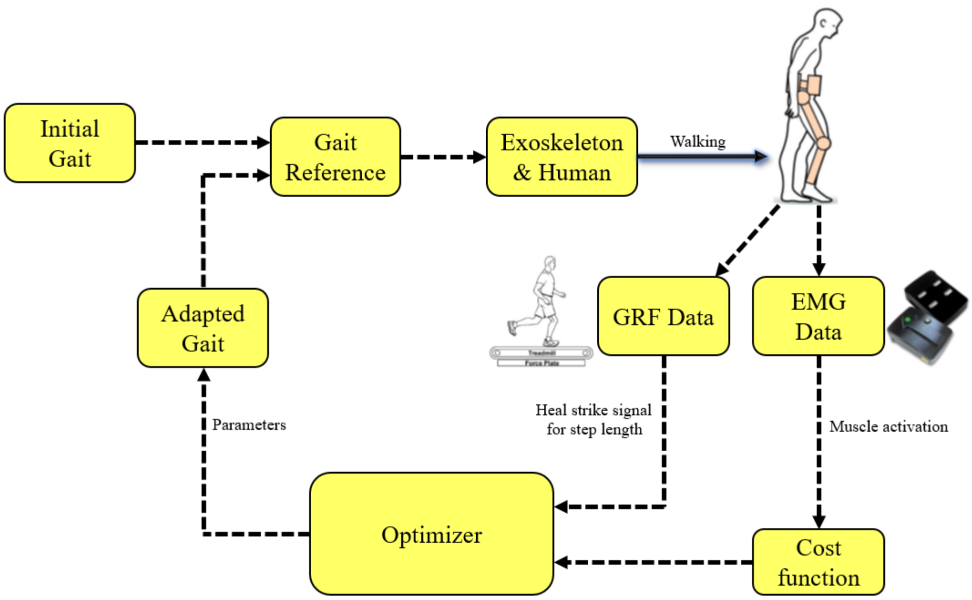


*Figure 18: Block diagram for the control algorithm to adapt to the gait pattern.*

In this control strategy with its multiple nested loops, the cost function generated from the muscle activation data by EMG and the ground reaction force (GRF) data used for gait cycle detection, are used to close the loop by way of the optimizer. This cost function based on EMG data is shown in Equation 3.1. The raw EMG data was rectified and filtered using the second-order Butterworth filter method and integrated over a time taken for *n* number of gait cycles:

$$J = \int_0^{t_n} |x(t)|\, dt \tag{3.1}$$

where $J$ is the cost function, $x(t)$ is the EMG value at time $t$, and $t_n$ is time taken for $n$ number of gait cycles.

To change the pattern of reference trajectory and duration of the gait cycle for walking, the user can do so in two ways: taking a greater number of steps in a sample time (reduce the duration of each step), and taking longer steps (change the pattern of the gait or increase amplitude of the trajectory). Based on the GRF data, heel strikes of the gait are detected, and the time taken for each gait was calculated; this data was given to the optimizer, which enabled the controller to change the speed of walking by controlling the number of time steps taken for each gait cycle. The optimizer generates parameters to minimize the cost function; and these parameters close the control loop, which can optimize the step length and the pattern of the gait cycle. Since the muscle activations are function of unknown parameters, a model-free optimization method, extremum seeking control (ESC) [44], was used to generate these parameters. ESC is described below.

### 3.3 Extremum Seeking Control (ESC)

Extremum Seeking Control (ESC), also called "self-optimizing control," has been used since the 1950s [45] [46], and the appearance of ESC dates back to 1922 [47] as a model-independent approach to optimization. ESC has been widely used in tuning and optimization in many applications with unknown parameters and uncertainties [48], such as power optimization for photovoltaic micro-converters [49], control of a thermoacoustic cooler [50] in which its performance is optimized, and stabilization of nonlinear dynamical systems with parametric uncertainties [51]. A detailed review of ESC development from 1922 to 2010 has been described in the prior research [52] [48].

Recently, ESC has been used to control the stiffness of a quasi-passive ankle exoskeleton [7] to reduce the muscular effort of human walking with an ankle exoskeleton using real-time optimization. The block diagram of ESC is shown in Figure 19, which finds the optimum points to minimize or maximize the objective function. This ESC adds a dither signal or periodic perturbation with small amplitude $\sin \omega t$ on the parameter command. Based on these changes in parameter, the cost function is measured with respect to the parameter. During this continuous process, the ESC detects the amount of parameter change that is needed in order to minimize the cost function.

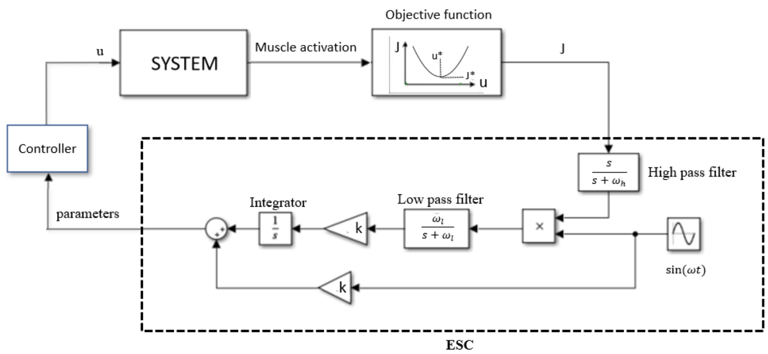


*Figure 19: Block diagram for implementation of extremum seeking control algorithm.*

### 3.4 Setup for the Real-Time Test

The Indego personal exoskeleton by Parker Hannifin, which supports individuals with spinal cord injury by enabling functional independence and upright mobility [9], was used in this research. The Indego was used to develop the control strategy that adapts the gait of the exoskeleton to the user's walking pattern. A human-in-the-loop control algorithm was designed in MATLAB/Simulink, based on the model provided by Parker Hannifin, as shown in Figure 3; and it was tested using real-time Simulink with the Indego using CAN bus to establish communication.

To test the controls algorithm during this research, the walking test with the Indego (Figure 20[a]) was performed on the instrumented treadmill. A split-belt, instrumented treadmill (VG005-A, Motek Medical, Amsterdam, Netherlands) [53] (Figure 20[b]) embedded with force plates that measure the ground reaction force (GRF) data was used for this research. The embedded force-plate sensor measures the forces and moments on the three axes for both left and right belts of the treadmill, which transfers data in 12 analog channels. The belt speed of this instrumented treadmill is controlled using the software D-Flow 3.16.2 by Motek Medical.

To measure the muscle activation of the user while walking with the exoskeleton, electromyography (EMG) sensors were used. An EMG sensor records the change in electric potential of the muscle by means of a surface electrode or needle electrodes [54]. For this test setup, the Trigno™ EMG sensors from DELSYS [55] (Figure 20[c]) were used, which measure muscle activations with surface electrodes.

The National Instruments data acquisition board PCI-6014 with 16 channels was used to send the analog data signals to the Simulink Desktop Real-Time Analog Input block. This block was used to close the controls loop in Simulink to achieve optimization. The GRF data was sent via 12 of the 16 analog channels, and the EMG data was sent in the remaining 4 of the 16 analog channels.

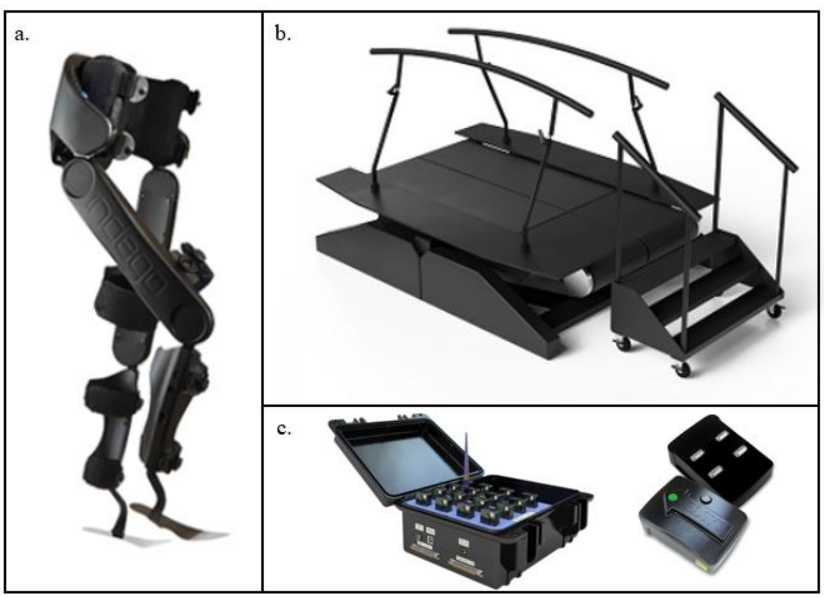


*Figure 20: a. The Indego exoskeleton [9]; b. Split-belt instrumented treadmill (VG005-A, Motek Medical) [53]; and c. Trigno™ EMG sensors from DELSYS [55].*

### 3.5 Optimization of Gait Cycle

To synchronize the exoskeleton and the user, the reference gait of the exoskeleton was optimized to adapt to the user's walking pattern while walking with the exoskeleton. This model-based controller was designed in MATLAB/Simulink, and the layout is shown in Figure 21. This model initializes the standard gait trajectories of right hip, right knee, left hip, and left knee at slow, normal, and fast speeds from David Winter's book [56] and takes the GRF data from the treadmill, the muscle activation data from the EMGs, and a user-defined number *n* that tells the algorithm to optimize every *n* number of gait cycles. The optimization of the gait cycle was done by the parameters from the optimizer as a continuous process that changes the reference trajectories given to the actuators of the exoskeleton in real time.

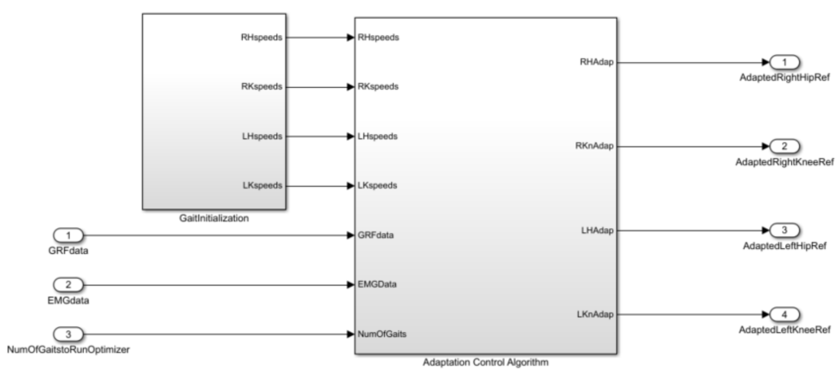


*Figure 21: Overview of the Adaptation Control algorithm designed in MATLAB/Simulink.*

This optimization is a two-part process. The first part detects the time taken for each step, based on the GRF data, selects the suitable speed of walking, and switches the gait patterns accordingly. For the second part, the optimizer generates parameters that modify the gait pattern by optimizing the objective function, based on muscle activation data from EMG sensors integrated over *n* number of gait cycles. Since the optimization of the generated cost function is based on muscle activations, and these muscle activations are a function of unknown parameters, a model-free optimization method ESC [44] was used to generate these parameters.

### 3.6 Preliminary Adaptation Test with one Joint and one Parameter

To test this control algorithm, a preliminary test was conducted. The control algorithm, shown in Figure 22, was implemented on one joint of the Indego exoskeleton, and a simple sine wave adaptation was tested with that joint using the optimizer and one parameter. The Indego exoskeleton was secured in a stand and a sine wave with a fixed amplitude was given as the reference angle trajectory to the left hip joint of the Indego exoskeleton while other joints were kept locked at zero position. As the left leg of the Indego oscillated following the reference trajectory, the amplitude of the oscillation was altered by physically pushing it to the new range of motion. During this process, the EMG sensors measured muscle activations at the biceps while the user tried to change the motion, and a cost function based on this muscle activation data was sent to the optimizer. The optimizer with ESC generated a parameter that changes the amplitude of the reference sine wave, in order to minimize the muscle activation. In this continuous process, the ESC generates the parameter that adapts the motion of the reference to the desired trajectory where muscle activation is minimal.

This test shows that the reference trajectory for the left hip actuator of the Indego exoskeleton adapted to the change in amplitude of the oscillations, which verifies the performance of the ESC-based optimizer. In this test, the initial or actual reference given to the actuator had an amplitude of 20 degrees, and the user tried to increase the amplitude of limb oscillations. As a result, the cost function based on EMG data integration was increased. To minimize this cost function, the optimizer changed the parameters, which in turn adapted the reference trajectory of the actuator. As a continuous process, muscle activation decreased while the actuator still maintained the adapted reference. The plots from these test results are shown in Figure 23.

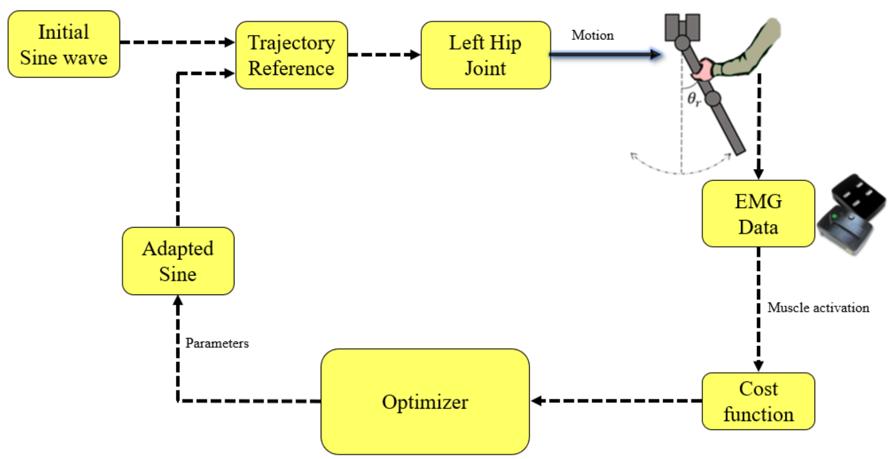


*Figure 22: Control algorithm for a preliminary test to adapt the motion in one joint using one parameter.*

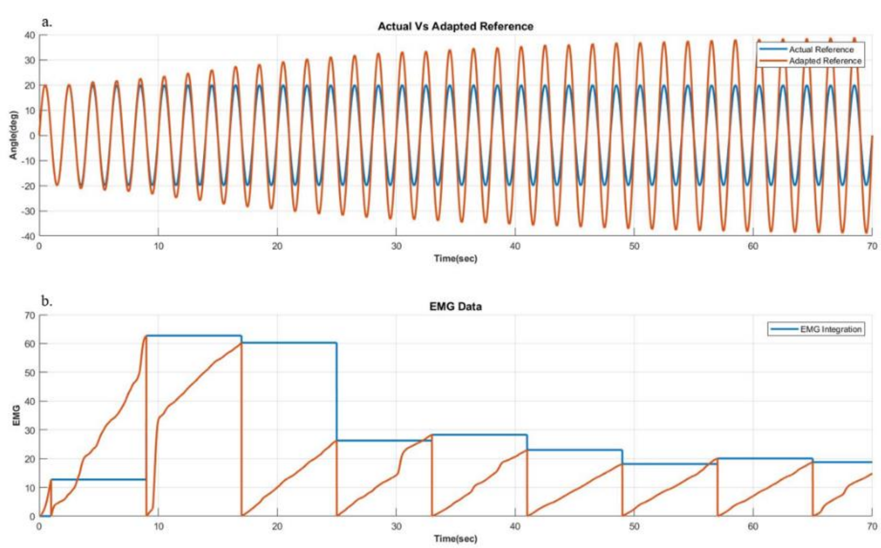


*Figure 23: Preliminary one joint test results with one parameter optimization. 23a. The actual and adapted reference trajectory; and 23b. The EMG data integration showing the decrease in muscle activation as the amplitude of the reference trajectory was increased*

### 3.7 Adaptation Test While Walking with the Indego

After the preliminary test on one joint with one-parameter optimization verified the performance of the control algorithm, a full walking test was performed to demonstrate the adaptation of the gait cycle trajectory of the Indego exoskeleton. The control algorithm shown in Figure 16 was implemented while walking on the instrumented treadmill with the Indego exoskeleton, and the EMG sensors monitored muscle activations. This algorithm has multiple nested loops based on GRF data and EMG data from the rectus femoris, as described in Sections 3.2 and 3.4, to perform respective tasks. The framework of the controls algorithm to adapt the gait of the Indego was based on optimizing the joint angle trajectories of actuators, as shown in Figure 24.

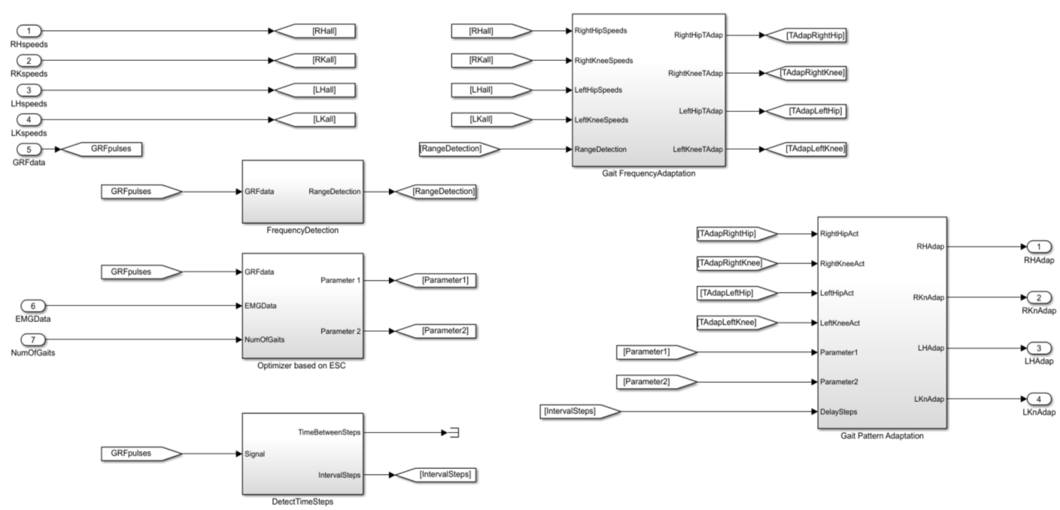


*Figure 24: Framework of the control algorithm to adapt gait reference trajectories of actuators in the Indego.*

During the test, the parameters were generated by the optimizer based on ESC and used to adapt the pattern of reference trajectories for each joint independently, using the adaptation algorithm based on the weighted average in the gait pattern adaptation block, as shown in Figure 25. The detailed view of the gait pattern algorithm block and its subsystems designed in MATLAB/Simulink are shown in Figure 25. Also, the gait frequency adaptation block adapted the speed changes based on GRF data. From this GRF data, the time and the number of time steps between each heel strike were measured. In the gait frequency adaptation algorithm, the range of frequencies is matched with a suitable speed and given as a base reference signal.

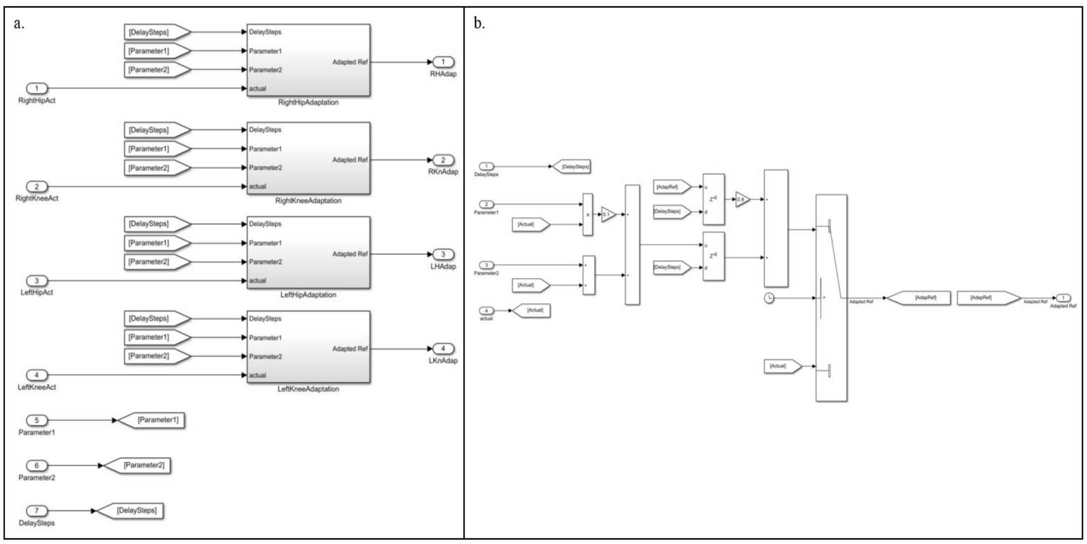


*Figure 25: a. Gait pattern adaptation algorithm subsystem, and b. Adaptation algorithm subsystem for each actuator.*

The results of this test with adaptation of the walking pattern and EMG integration are shown in Figure 26. In this walking test, it is clearly evident that the adaptation algorithm is changing the pattern of the gait reference trajectory as well as the frequency of walking while reducing the muscle activations. This shows the performance of the control algorithm in maintaining an equilibrium between the user and the exoskeleton. Figure 27 shows a zoomed-in plot of actual versus adapted reference to illustrate the adaptation of the walking pattern and the frequency.

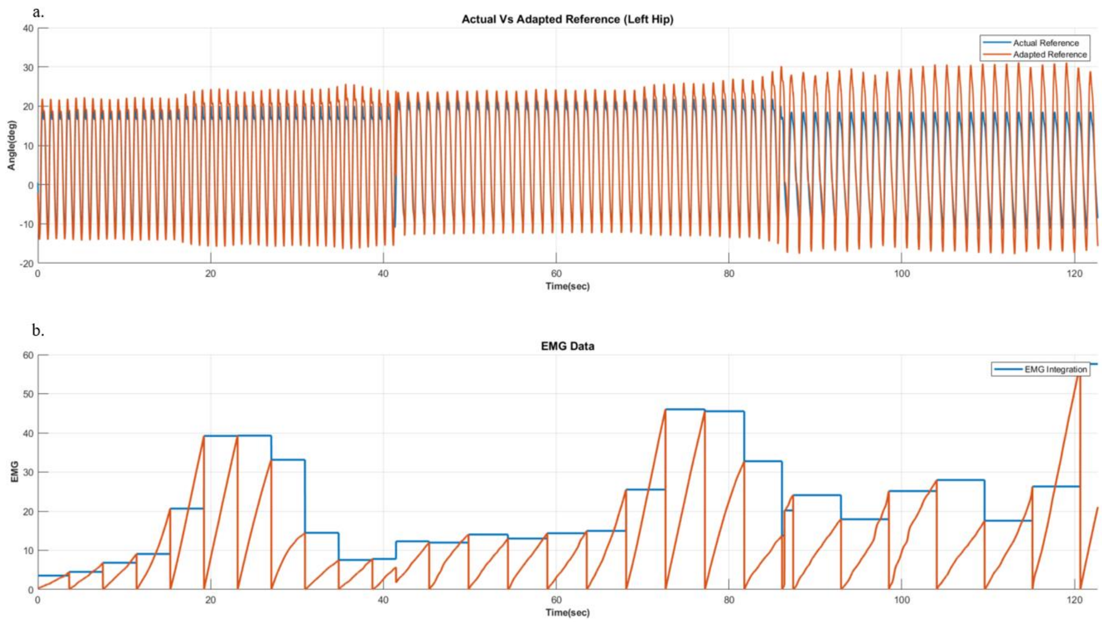


*Figure 26: Adaptation algorithm testing while walking with Indego exoskeleton. 26a. The actual and adapted reference trajectory, and 26b. The EMG data integration.*

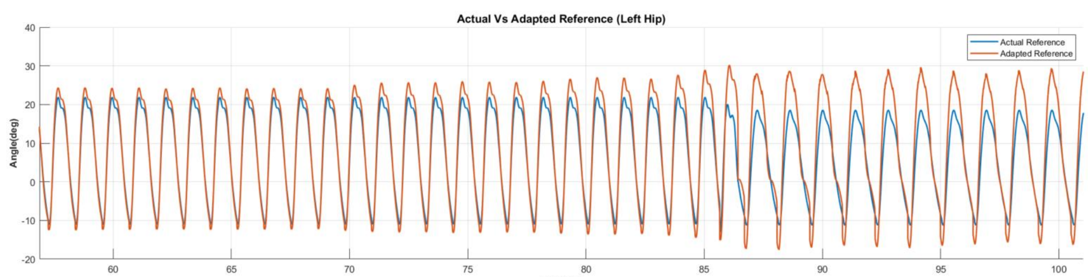


*Figure 27: Actual and adapted reference to show the pattern and frequency adaptation of the Indego exoskeleton.*

### 3.8 Discussion

In this chapter, an optimization-based control system model was designed to adapt the walking pattern of the Indego exoskeleton to changes in the user's walking. This controller was designed based on a model-free optimizer extremum seeking controller (ESC). When a user changes the walking pattern, the coordination between the user and the exoskeleton is altered, which increases muscle activations. A cost function based on muscle activations, as measured by the EMG sensor, is optimized by the ESC providing parameters. Based on these parameters, the adaptation algorithm modified the joint reference trajectories of the Indego exoskeleton's actuators to minimize muscle activation while the user walks.

This algorithm also inputs the ground reaction force data to calculate the gait cycle duration. The adaptation rate can be modified by the user by specifying the number of gait cycles for which the algorithm should adapt the walking pattern. This algorithm can adapt to both the pattern of the reference trajectory and the duration of the gait cycle or walking speed. Real-time test results show the effectiveness of the controls in adapting to different patterns of walking.

# CHAPTER IV

# CONCLUSIONS AND DISCUSSION

## 4.1 Conclusions

The two aims of this thesis were to design a controller to improve balance in the underactuated Indego exoskeleton and to make the Indego exoskeleton adapt to the different walking patterns of its users.

The first aim was achieved by designing and implementing a control algorithm to improve the balance of the Indego. The simulation results demonstrate the effectiveness of the proposed control algorithm, based on the LQR method, in balancing the underactuated exoskeleton. Its performance was further improved by 25% through optimizing the control gain matrix using the Nealder-Mead simplex method. From these results, it is evident that a small change in the optimized control gain matrix resulted in improved performance.

The second aim was achieved by designing and testing an optimization-based control system model to adapt the pattern of the Indego exoskeleton to the changes in the user’s walking. This controller was designed based on a model-free optimizer extremum seeking controller (ESC). The experimental results show the effectiveness of this controller in adapting the Indego to changes in the pattern and speed of walking.

### 4.2 Future Work

In the future, the controller designed and simulated to improve the balance in the underactuated exoskeleton can be implemented on a test bed in real time. Also, the controller can be tested for robustness with added external disturbances. As the performance of the system is sensitive to small changes in system parameters, the sensitivity of the system with changes in control parameters can be further studied. Also, the sensitivity of the system to physical modeling can be studied. There is also a scope improve balance capabilities, such as improved range of initial position grid and sensitivity to system parameters in exoskeletons by using advanced techniques such as trajectory optimization, artificial intelligence, or using non-linear controllers including sliding mode control and model predictive controllers. The controller can also be optimized based on human data, using real-time optimization. Since Indego exoskeleton does not have an actuator and a sensor at its ankle joint, a position and velocity sensor can be integrated into the exoskeleton for the full state feedback of the ankle joint.

The effectiveness of the controller in making the exoskeleton adapt to the user's walking patterns and speed can be statistically analyzed with various walking patterns of multiple test subjects. Also in the future, EMG data from multiple muscles can be combined to form a complex cost function, and it can be optimized using real-time optimizers, such as machine learning or deep reinforcement learning techniques. Also, to implement these controls in the commercialized exoskeletons like Indego, force sensors that use dynamic resistance to calculate the applied force, such as Ohmite FSR [57] could be used to detect heal strikes and duration of gait cycles, and EMG sensors such as Muscle Sensor Surface EMG Electrodes [58] could be used to measure the muscle activation of the user. These sensors can be integrated with the existing exoskeleton devices to add these control features.

By adding these new features to the control architecture of the exoskeletons, it is important to study safety involved with using these controllers and switching between the controllers based on the task. To study the safety of these controllers, failure mode and effects criticality analysis can be performed. With the advancement in embedded software controls, functional safety can be programmed in order to prevent any failures of the control modes by taking the system to a pre-defined safe state mode.

## REFERENCES


[1] H. Herr, "Exoskeletons and orthoses: classification, design challenges and future directions," *Journal of NeuroEngineering and Rehabilitation,* 2009.

[2] N. Yagn, "Apparatus for facilitating walking, running, and jumping". USA Patent US420179A, 28 Jan 1890.

[3] D. John and E. Eric, "Human bipedal locomotion device". U.S. Patent 5,016,869, 1990.

[4] T. Bosch, J. Van Eck, K. Knitel and M. De Looze, "The effects of a passive exoskeleton on muscle activity, discomfort and endurance time in forward bending work," *Applied Ergonomics,* vol. 54, pp. 212-217, 2016.

[5] "Skyrunners," Skyrunner Australia, [Online]. Available: http://skyrunneraustralia.com.au/page.html?id=1. [Accessed 25 06 2021].

[6] M. Bobby, "Types And Classifications of Exoskeletons," Exoskeleton Report, 19 August 2015. [Online]. Available: https://exoskeletonreport.com/2015/08/types-and-classifications-of-exoskeletons/. [Accessed 06 June 2021].

[7] K. Saurav, M. R. Zwall, E. A. Bolivar-Nieto, R. D. Gregg and N. Gans, "Extremum Seeking Control for Stiffness Auto-Tuning of a Quasi-Passive Ankle Exoskeleton," *IEEE Robotics and Automation Letters, vol. 5, no. 3,* pp. 4604-4611, July 2020.

[8] "Spinal Cord Injury Facts and Figures at a Glance," 01 June 2021. [Online]. Available: https://www.nscisc.uab.edu/Public/Facts%20and%20Figures%20-%202021.pdf.

[9] "INDEGO EXOSKEETON," Parker Hannifin, [Online]. Available: http://www.indego.com/indego/us/en/home. [Accessed 06 2021].

[10] A. Esquenazi, M. Talaty, A. Packel and M. Saulino, "The rewalk powered exoskeleton to restore ambulatory function to individuals with thoracic-level motor-complete spinal cord injury," *American Journal of Physical Medicine & Rehabilitation,* vol. 91, no. 11, pp. 911-921, 2012.

[11] K. Jinsoo, L. Guik, H. Roman, A. R. Dheepak, K. Nikos, N. Danielle, G. Ignacio, E. Asa, M. Patrick, P. David, M. Nicolas, K. C. Dabin, M. Philippe and W. J. Conor, "Reducing the metabolic rate of walking and running with a versatile, portable exosuit," *Science,* vol. 365, no. 6454, pp. 668-672, 2019.

[12] H. Kazerooni and R. Steger, "The Berkeley Lower Extremity Exoskeleton," *Journal of Dynamic Systems, Measurement, and Control,* vol. 128, no. 1, pp. 14-25, 2005.

[13] S. Rudolf, P. Florian and R. David, "Hydraulic actuation of exoskeletons - state of the art and prospects," *International Robotics & Automation Journal,* vol. 4, no. 1, p. 96, 2018.

[14] G. Justin, S. Ryan and H. Kazerooni, "Control and system identification for the Berkeley lower extremity exoskeleton (BLEEX)," *Advanced Robotics,* vol. 20, pp. 989-1014, 2006.

[15] H. Quintero, R. J. Farris and M. Goldfarb, "“A method for the autonomous control of lower limb exoskeletons for persons with paraplegia," *Journal of Medical Devices,* vol. 6, p. 0410031–0410036, 2012.

[16] A. Blake, K. Morgan and M. Bendall, "Falls by elderly people at home: Prevalence and associated factors," *AGE AND AGEING,* vol. 17, no. 6, pp. 365-372, 1988.

[17] M. J. P. Pavol, T. M. Owings, K. T. M. Foley and M. D. P. Grabiner, "Influence of Lower Extremity Strength of Healthy Older Adults on the Outcome of an Induced Trip," *Journal of the American Geriatrics Society,* vol. 50, no. 2, pp. 256-262, 2002.

[18] "INDEGO PERSONAL EXOSKELETON," Parker Hannifin, [Online]. Available: http://www.indego.com/indego/us/en/indego-personal.

[19] R. J. Farris, "DESIGN OF A POWERED LOWER-LIMB EXOSKELETON AND CONTROL FOR GAIT ASSISTANCE IN PARAPLEGICS," *Dissertation submitted for DOCTOR OF PHILOSOPHY at Vanderbilt University,* 2012.

[20] H. A. Quintero, R. J. Farris, K. Ha and M. Goldfarb, "Preliminary Assessment of the Efficacy of Supplementing Knee Extension Capability in a Lower Limb Exoskeleton with FES," in *34th Annual International Conference of the IEEE EMBS,* San Diego, California USA,, 2012.

[21] "Indego Personal Brochure," [Online]. Available: http://www.indego.com/indego/us/en/indego-personal.

[22] S. R. Bonifacio, O. O. Patricio and P. G. Alexander, "Robust Stabilizing Control for the Electromechanical Triple-Link Inverted Pendulum System," *International Federation of Automatic Control,* p. 314–319, 2018.

[23] S. Kajita and K. Tani, "Study of dynamic biped locomotion on rugged terrain-derivation and application of the linear inverted pendulum mode," *Robotics and Automation, 1991 IEEE International Conference,* vol. 2, pp. 1405-1411.

[24] A. Elhasairi and A. Pechev, "Humanoid Robot Balance Control Using the Spherical Inverted Pendulum Mode," *Frontiers in Robotics and AI* , vol. 2, 2015.

[25] Y. Wang, Q. Zhu, R. Xiong and J. Chu, "Standing Balance Control for Position Control-Based Humanoid Robot," in *3rd IFAC International Conference on Intelligent Controland Automation Science*, Chengdu, China, 2013.

[26] C. Keil, "2D Dynamic Simulations," [Online]. Available: https://www.colinkeil.com/2d-dynamics-simulations. [Accessed 28 June 2021].

[27] R. Dvorak, F. F and K. Jurgen, Chaos and Stability in Planetary Systems, ISBN 3540282084, 2005.

[28] B. Torby, "Energy Methods". Advanced Dynamics for Engineers, CBS College Publishings, ISBN 0-03-063366-4., 1984.

[29] "Lagrangian mechanics," Scientific Library, [Online]. Available: http://www.scientificlib.com/en/Physics/LX/LagrangianMechanics.html. [Accessed 28 06 2021].

[30] R. Tedrake, "Underactuated Robotics: Algorithms for Walking, Running, Swimming, Flying, and Manipulation," MIY, [Online]. Available: http://underactuated.mit.edu/. [Accessed 2021 29 06].

[31] S. Sehgal and S. Tiwari, "LQR Control for Stabilizing Triple Link Inverted Pendulum System," in *International Conference on Power, Control and Embedded Systems*, 2012.

[32] J. C. Lagarias, J. A. Reeds, M. H. Wright and P. E. Wright, "CONVERGENCE PROPERTIES OF THE NELDER–MEAD SIMPLEX METHOD IN LOW DIMENSIONS," *Society for Industrial and Applied Mathematics Journal of Optimization*, vol. 9, no. 1, pp. 112-147, 1998.

[33] W. H. Press, T. W. Vetterling and S. Teukolsky, "Section 10.5. Downhill Simplex Method in Multidimensions," in *Numerical Recipes: The Art of Scientific Computing (3rd ed.).*, New York, Cambridge University Press, 2007.

[34] H. Huang, J. Si, A. Brandt and M. Li, "Taking Both Sides: Seeking Symbiosis Between Intelligent Prostheses and Human Motor Control during Locomotion," *Current Opinion in Biomedical Engineering,* 2021.

[35] B. L. Fylstra, I.-C. Lee, S. Huang, A. Brandt, M. D. Lewek and H. Huang, "Human-prosthesis coordination: A preliminary study exploring coordination with a powered ankle-foot prosthesis," *Clinical Biomechanics,* vol. 80, 2020.

[36] H. Kawamoto, S. Lee, S. Kanbe and Y. Sankai, "Power Assist Method for HAL-3 using EMG-based Feedback Controller," *Systems, man and cybernetics, 2003. IEEE international conference,* vol. 2, no. 2, pp. 1648-1653.

[37] H. H. Kevin, S. A. Murray and M. Goldfarb, "An Approach for the Cooperative Control of FES With a Powered Exoskeleton During Level Walking for Persons With Paraplegia," *IEEE transactions on neural systems and rehabilitation engineering: a publication of the IEEE Engineering in Medicine and Biology Society,* pp. 455-466, 2015.

[38] J. Zhang, P. Fiers, K. A. Witte, R. W. Jackson, K. L. Poggensee, C. G. Atkeson and S. H. Collins, "Human-in-the-loop optimization of exoskeleton assistance during walking," *Science,* pp. 1280--1284, 2017.

[39] R. M. Alexander, "Optimization and Gaits in the Locomotion of Vertebrates," *PHYSIOLOGICAL REVIEWS* , vol. 69, no. 4, pp. 1199-1227, 1989.

[40] M. L. Handford and M. Srinivasan, "Robotic lower limb prosthesis design through simultaneous computer optimizations of human and prosthesis costs," *SCIENTIFIC REPORTS*, vol. 6, 2016.

[41] W. Felt, J. C. Selinger, M. J. Donelan and D. C. Remy, ""Body-In-The-Loop": Optimizing Device Parameters Using Measures of Instantaneous Energetic Cost," *PLOS ONE*, vol. 10, 2015.

[42] M. Srinivasan and A. Ruina, "Computer optimization of a minimal biped model discovers walking and running," *Nature*, vol. 439, pp. 72-75, 2006.

[43] A. Schmitz, A. Silder, B. Heiderscheit, J. Mahoney and D. G. Thelen, "Differences in lower-extremity muscular activation during walking between healthy older and young adults," *Journal of Electromyography and Kinesiology*, vol. 19, pp. 1085-1091, 2009.

[44] K. B. Ariyur and M. Krstić, Real-Time Optimization by Extremum-Seeking Control, Hoboken, NJ, USA: Wiley, 2003.

[45] C. S. Draper and Y. T. Li, Principles of optimalizing control systems and an application to the internal combustion engine, New York: American Society of Mechanical Engineers, 1951.

[46] P. F. Blackman, " Extremum-seeking regulators," in *An exposition of adaptive control*, New York, The Macmillan Company, 1962.

[47] M. Leblanc, "Sur l'electri"cation des chemins de fer au moyen de courants alternatifs de frequence elevee," *Revue Generale de l'Electricite,* 1922.

[48] A. Scheinker and D. Scheinker, "Extremum Seeking for Stabilization of Systems Not Affine in Control," *International Journal of Robust and Nonlinear Control*, 2017.

[49] A. Ghaffari, M. Krstic and S. Seshagiri, "Power optimization for photovoltaic micro-converters using multivariable Newton-based extremum seeking," *IEEE Transactions on Control Systems Technology*, vol. 22, pp. 2141-2149, 2014.

[50] Y. Li, M. Rotea, G. Chiu, L. Mongeau and I. Paek, "“Extremum seeking control of a tunable thermoacoustic cooler," *IEEE Transactions on Automatic Control*, vol. 13, pp. 527-536, 2005.

[51] M. Guay and T. Zhang, "Adaptive extremum seeking control of nonlinear dynamics systems with parametric uncertainties," *Automatica*, vol. 39, pp. 1283-1293, 2003.

[52] W. H. Moase, C. Manzie, D. Nesic and I. Y. Mareels, "Extremum seeking from 1922 to 2010," in *29th Chinese Control Conference*, Beijing, China, 2010.

[53] "Motek M-Gait," Summit Medical & Scientific, [Online]. Available: https://summitmedsci.co.uk/products/motek-mgait/. [Accessed 2021 07 07].

[54] "Electromyography MeSH Descriptor Data 2021," U.S. National Library of Medicine, 01 01 1999. [Online]. Available: https://meshb.nlm.nih.gov/record/ui?name=Electromyography. [Accessed 09 07 2021].

[55] "Delsys Trigno™ Wireless EMG System," JALI MEDICAL, [Online]. Available: https://www.jalimedical.com/delsys-trigno-wireless-emg-system.php. [Accessed 07 07 2021].

[56] D. A. Winter, The Biomechanics and Motor Control of Human Gait: Normal, Elderly and Pathological, Universithy of Waterloo Press, 1993.

[57] "FSR Series OHMITE," [Online]. Available: https://www.mouser.com/datasheet/2/303/res_fsr-1590094.pdf. [Accessed 10 08 2021].

[58] "Muscle Sensor Surface EMG Electrodes - H124SG Covidien," Adafruit, [Online]. Available: https://www.adafruit.com/product/2773#technical-details. [Accessed 10 08 2021].

[59] K. Saurav, M. Alireza, D. Quintero, R. Saivash, G. Nicholas and G. Robert, "Extremum Seeking Control for Model-Free Auto-Tuning of Powered Prosthetic Legs," *IEEE Transactions on Control Systems and Technology,* vol. 28, no. 6, pp. 1-16, 2019.

[60] Reinkensmeyer, M.-C. Laura and D. J, "Review of control strategies for robotic movement training after neurologic injury," *Journal of NeuroEngineering and Rehabilitation,* 2009.

[61] S. Srivastava, P. Kao, S. Kim, P. Stegall, D. Zanotto, J. Higginson, S. Agrawal and J. Scholz, "Assist-as-Needed Robot-Aided Gait Training Improves Walking Function in Individuals Following Stroke," *IEEE Trans Neural Syst Rehabil Eng,* vol. 23, pp. 956-963, 2015.

[62] S. Kumar, A. Mohammadi, D. Quintero, S. Rezazadeh, N. Gans and R. Gregg, "Extremum Seeking Control for Model-Free Auto-Tuning of Powered Prosthetic Legs," *IEEE Transactions on Control Systems Technology,* vol. 28, no. 6, pp. 2120-2135, 2020.

[63] L. Peternel, T. Noda, U. A. Petrič T, J. Morimoto and J. Babič, "Adaptive Control of Exoskeleton Robots for Periodic Assistive Behaviours Based on EMG Feedback Minimisation," *PLOS ONE,* vol. 11, pp. 1-26, 2016.

APPENDIX

```
% Matlab code to derive the dynamic equations of the 3-link pendulum
% using the Lagrangian method, and formulate the system dynamics in
% state space form: dx/dt = f(x,u)

   clear global          % To make sure nothing left over from before
   global xdotfun        % function with the equations of motion
   global ankle          % ankle properties (needed in odefun)

   % model parameters
   g = 9.81;                        % gravity
   ms=10; mth=18; mh=45;            % masses of the 3 links
   I1=0.13; I2=0.32; I3=3.83;     % moment of inertia
   d1=0.25; d2=0.35; d3=0.35;      %
   L1=0.45; L2=0.45;                % Length of the links
   ankle.k = 200;    % Nm/rad, stiffness of the passive ankle joint
   % ankle torque (acting on leg) must stay roughly beween -dheel*mg
   % and dtoe*mg, otherwise the foot will rotate (free body diagram of
   % foot explains this)
   dheel = 0.06;    % horizontal distance (m) heel to ankle
   dtoe  = 0.24;    % horizontal distance (m) ankle to toe
   ankle.umin = -dheel*(ms+mth+mh)*g;
   ankle.umax =   dtoe*(ms+mth+mh)*g;

   % motion variables and joint torques
   syms q1 q2 q3 q1dot q2dot q3dot q1ddot q2ddot q3ddot
   syms u1 u2 u3
   q = [q1 ; q2 ; q3];
   qdot = [q1dot ; q2dot ; q3dot];
   qddot = [q1ddot ; q2ddot ; q3ddot];
   u = [u1;u2;u3];

   % forward kinematics
   % q1 is zero when link 1 is vertical.  q2 and q3 are relative
   % angles
   x1 = d1*cos(pi/2+q1);
   y1 = d1*sin(pi/2+q1);
   x2 = L1*cos(pi/2+q1) + d2*cos(pi/2+q1+q2);
   y2 = L1*sin(pi/2+q1) + d2*sin(pi/2+q1+q2);
   x3 = L1*cos(pi/2+q1) + L2*cos(pi/2+q1+q2) + d3*cos(pi/2+q1+q2+q3);
   y3 = L1*sin(pi/2+q1) + L2*sin(pi/2+q1+q2) + d3*sin(pi/2+q1+q2+q3);

   % velocities of the links, using chain rule
   vx1 = diff(x1,q1)*q1dot;
   vy1 = diff(y1,q1)*q1dot;
   vx2 = diff(x2,q1)*q1dot + diff(x2,q2)*q2dot;
   vy2 = diff(y2,q1)*q1dot + diff(y2,q2)*q2dot;
   vx3 = diff(x3,q1)*q1dot + diff(x3,q2)*q2dot + diff(x3,q3)*q3dot;
   vy3 = diff(y3,q1)*q1dot + diff(y3,q2)*q2dot + diff(y3,q3)*q3dot;

   % kinetic energy T, potential energy V
   T = ( ms*(vx1^2 + vy1^2) + I1*q1dot^2 + ...
        mth*(vx2^2 + vy2^2) + I2*(q1dot+q2dot)^2 + ...
        mh*(vx3^2 + vy3^2) + I3*(q1dot+q2dot+q3dot)^2 ) / 2;
```

```
    V = ms*g*y1 + mth*g*y2 + mh*g*y3 ;

    % if there is a horizontal acceleration a of the floor,
    % this acts exactly like a horizontal gravitational field
    % a is defined positive when the floor accelerates in the positive
x
    % direction
    syms a
    V = V + ms*a*x1 + mth*a*x2 + mh*a*x3 ;

    % define Lagrangian L, and form the components of the Lagrange
    % equation
    L = T-V
    DLDqdot = gradient(L, qdot);                        % dL/dqdot
    ddtDLDqdot = jacobian(DLDqdot,qdot)*qddot ...       % d/dt of dL/dqdot
               + jacobian(DLDqdot,q)*qdot;
    DLdq = gradient(L, q);                              % dL/dq

    % Lagrange equation is: d/dt(dL/dqdot) - dL/dq = u
    % Form the left hand side (LHS) as a 3x1 matrix (LHS)
    LHS = ddtDLDqdot - DLdq;
    LHS = simplify(LHS)

    % getting the equation of motion in this form: M(q)*qdd + C(q,qd) =
u
    % find M(3x3) and C(3x1), and solve qdd
    M = simplify(jacobian(LHS, qddot))
    C = simplify(LHS - M * qddot)
    qddot = M\(u-C);    % solves qddot symbolically from equations of
motion

    % define state variables x and create a function that computes xdot
    syms x1 x2 x3 x4 x5 x6
    x = [x1;x2;x3;x4;x5;x6];
    q1    = x1; q2    = x2; q3    = x3;
    q1dot = x4; q2dot = x5; q3dot = x6;
    xdot = [qdot; qddot];
    xdot = subs(xdot);  % substitutes x for q and qdot
    xdotfun = matlabFunction(xdot, 'File', 'xdotfun.m');

    % linearize the dynamics at x=0, in the form xdot = A*x + B*u
    A = jacobian(xdot,x);
    B = jacobian(xdot,u);
    A(:,1) = A(:,1) - ankle.k * B(:,1);  % put ankle stiffness (u1 = -
    % k*x1) in A

    % substitute x=0 and a=0 in A and B, convert A and B to numbers
    x1 = 0; x2 = 0; x3 = 0; x4 = 0; x5 = 0; x6 = 0;
    a = 0;
    A = double(subs(A));
    B = double(subs(B));

    % To create the LQR controller
    B = B(:,2:3)            % removing column 1 (ankle torque) from B


%================================================================
```

```matlab
function [xdot] = odefun(t,x)
    global xdotfun perturb K ankle

    % horizontal acceleration of the floor
    a = interp1(perturb.t, perturb.a, t);

    % controller goes here
    u = [0; -K*x];  % torques from controller

    % add the passive ankle torque (limited between umin and umax)
    u(1) = -ankle.k * x(1); % passive ankle torque
    u(1) = max(ankle.umin, u(1));
    u(1) = min(ankle.umax, u(1));

    % add a passive spring/damper torque that resists knee motion when
    % angle goes negative
    if x(2) < 0
        u(2) = u(2) - 5000*x(2) - 200*x(5);
    end

    % use the state space (1st order) nonlinear dynamics function
    xdot = xdotfun(a,u(1),u(2),u(3),x(1),x(2),x(3),x(4),x(5),x(6));
end
```